Received: 12 August 2022 | Revised: 30 November 2022 | Accepted: 19 December 2022

DOI: 10.1002/alz.12970

Alzheimer's & Dementia®
THE JOURNAL OF THE ALZHEIMER'S ASSOCIATION

ALTERNATE FORMAT RESEARCH ARTICLE

Pathogenesis of Alzheimer's disease: Involvement of the choroid plexus

Maria Čarna[1] | Isaac G. Onyango[1] | Stanislav Katina[1,2] | Dušan Holub[3] | Jan Sebastian Novotny[1] | Marketa Nezvedova[4] | Durga Jha[4] | Zuzana Nedelska[1,5] | Valentina Lacovich[1] | Thijs Vande Vyvere[6] | Ruben Houbrechts[6] | Krystine Garcia-Mansfield[7] | Ritin Sharma[7] | Victoria David-Dirgo[7] | Martin Vyhnalek[1,5] | Kateřina Texlova[1] | Hernan Chaves[8] | Nadine Bakkar[9] | Lucia Pertierra[8] | Mojmir Vinkler[2] | Hana Markova[1,5] | Jan Laczo[1,5] | Kateřina Sheardova[1,10] | Marcela Hortova-Kohoutkova[1] | Jan Frič[1,11] | Giancarlo Forte[1] | Petr Kaňovsky[12] | Silvie Belaškova[1] | Jiři Damborsky[1,4] | Jakub Hort[1,5] | Nicholas T. Seyfried[13,14,15] | Robert Bowser[9] | Gustavo Sevlever[8] | Robert A. Rissman[16] | Richard A. Smith[17] | Marian Hajduch[3] | Patrick Pirrotte[7,18] | Zdenek Spacil[4] | Eric B. Dammer[13,14] | Clara Limbäck-Stokin[19,20] | Gorazd B. Stokin[1,21,22]

[1]International Clinical Research Centre, St. Anne's University Hospital, Brno, Czech Republic

[2]Institute of Mathematics and Statistics, Masaryk University, Brno, Czech Republic

[3]Institute for Molecular and Translational Medicine, Faculty of Medicine and Dentistry, Palacky University Olomouc, Olomouc, Czech Republic

[4]RECETOX Centre, Faculty of Sciences, Masaryk University, Brno, Czech Republic

[5]Memory Clinic, Department of Neurology, 2nd Faculty of Medicine, Charles University and Motol University Hospital, Prague, Czech Republic

[6]Icometrix, Leuven, Belgium

[7]Collaborative Center for Translational Mass Spectrometry, Translational Genomics Research Institute, Phoenix, Arizona, USA

[8]FLENI, Buenos Aires, Argentina

[9]Department of Neurobiology, Barrow Neurological Institute, Phoenix, Arizona, USA

[10]1st Department of Neurology, St. Anne's University Hospital and Faculty of Medicine, Masaryk University, Brno, Czech Republic

[11]Institute of Hematology and Blood Transfusion, Prague, Czech Republic

[12]Department of Neurology, Faculty of Medicine and Dentistry, Palacky University Olomouc and Research and Science Department, University Hospital Olomouc, Olomouc, Czech Republic

[13]Center for Neurodegenerative Disease, Emory University School of Medicine, Atlanta, Georgia, USA

[14]Goizueta Alzheimer's Disease Research Center, Emory University, Atlanta, Georgia, USA

[15]Departments of Bioachemistry and Neurology, Emory University School of Medicine, Atlanta, Georgia, USA

[16]Department of Neurosciences, University of California San Diego, La Jolla, California, USA

[17]Center for Neurologic Study, La Jolla, California, USA

[18]Mass Spectrometry & Proteomics Core Facility, City of Hope Comprehensive Cancer Center, Duarte, California, USA

[19]Department of Cellular Pathology, Imperial College Healthcare NHS Trust, London, UK

[20]Imperial College London, Faculty of Medicine, London, UK

[21]Division of Neurology, University Medical Centre, Ljubljana, Slovenia

[22]Translational Aging and Neuroscience Program, Mayo Clinic, Rochester, Minnesota, USA

Correspondence
Gorazd B. Stokin, International Clinical Research Centre, St. Anne's University Hospital, Brno, Czech Republic
Email: gbstokin@alumni.ucsd.edu

Present address
Clara Limbäck-Stokin, Neuropathology and Ocular Pathology Department, Oxford University Hospitals NHS Foundation Trust, Oxford, UK

Funding information
European Regional Development Funds, Grant/Award Number: CZ.02.1.01/0.0/0.0/16_019/0000868; The EU Horizon 2020, Grant/Award Numbers: 857560, CZ.02.1.01/0.0/0.0/17_043/0009632; THE Cetocoen Plus, Grant/Award Number: CZ.02.1.01/0.0/0.0/15_003/0000469; Czech Ministry of Health, Grant/Award Numbers: NV 18–04–00346, 18–04–00455, 00064203, 19–08–00472; Inbio, Grant/Award Number: CZ.02.1.01/0.0/0.0/16_026/0008451; NIH, Grant/Award Number: P30 AGO62429; Barrow Neurological Foundation and the Fein Foundation grant, Grant/Award Number: LM2018121; Grant Agency of the Masaryk University, Grant/Award Number: MUNI/G/1131/2017; National Cancer Institute of the NIH, Grant/Award Number: P30CA033572; NIA, Grant/Award Numbers: U01 U01AG061357, LX22NPO5107, 6980382

Abstract

The choroid plexus (ChP) produces and is bathed in the cerebrospinal fluid (CSF), which in aging and Alzheimer's disease (AD) shows extensive proteomic alterations including evidence of inflammation. Considering inflammation hampers functions of the involved tissues, the CSF abnormalities reported in these conditions are suggestive of ChP injury. Indeed, several studies document ChP damage in aging and AD, which nevertheless remains to be systematically characterized. We here report that the changes elicited in the CSF by AD are consistent with a perturbed aging process and accompanied by aberrant accumulation of inflammatory signals and metabolically active proteins in the ChP. Magnetic resonance imaging (MRI) imaging shows that these molecular aberrancies correspond to significant remodeling of ChP in AD, which correlates with aging and cognitive decline. Collectively, our preliminary *post-mortem* and in vivo findings reveal a repertoire of ChP pathologies indicative of its dysfunction and involvement in the pathogenesis of AD.

KEYWORDS
aging, Alzheimer's disease, cerebrospinal fluid, choroid plexus, pathology

Highlights

- Cerebrospinal fluid changes associated with aging are perturbed in Alzheimer's disease
- Paradoxically, in Alzheimer's disease, the choroid plexus exhibits increased cytokine levels without evidence of inflammatory activation or infiltrates
- In Alzheimer's disease, increased choroid plexus volumes correlate with age and cognitive performance

1 | NARRATIVE

1.1 | Contextual background

Alzheimer's disease (AD) manifests clinically with behavioral changes and progressive decline in cognitive faculties[1] and is by far the most common cause of dementia in the elderly.[2] Pathologically, AD brains exhibit synaptic and neuronal loss[3] accompanied by reactive glia.[4–7] Senile plaques and neurofibrillary changes are regarded as the disease-characterizing neuropathological hallmarks.[8] However, these hallmarks are observed also in people who are cognitively healthy[9,10] or suffer from different neurodegenerative disorders,[11] while lesions typical of other disorders such as α-synuclein inclusions frequently populate AD brains.[12] Despite this clinical and neuropathological spectrum of the Alzheimer's syndrome,[13] accumulating evidence suggests that the most proximal neurobiological event underlying clinical features involves impaired brain connectivity due to inadequate synaptic performance.[14–17] Accordingly, there is significant interest in understanding the neurobiology of synaptic failure in AD[18] and in particular its intimate relationship with neuroinflammation.[17,19] Since the choroid plexus (ChP) plays a pivotal role in brain homeostasis including its immune status,[20–22] we here preliminarily investigate structural health of the ChP and provide early evidence of complex ChP pathology indicative of its dysfunction in patients with AD.

The discovery that genetic defects segregating with kindreds afflicted by familial AD (FAD)[23] perturb formation of amyloid-β peptides (Aβ), the major constituents of senile plaques,[24] paved the way to the amyloid hypothesis. This posits that aberrant Aβ underlie the pathogenesis of AD.[25] Although clinical trials have failed to provide definitive support for the amyloid hypothesis,[26] the recognition that FAD mutations impair numerous cellular processes ranging from endosomal activity to axonal transport[27,28] indicates that, in the

foreseeable future, the mechanisms by which FAD mutations cause AD will ultimately be deciphered. The vast majority of AD cases, however, are sporadic in nature and mechanisms at play go beyond those underlying the pathogenesis of FAD. The major risk factor of sporadic AD is aging,[29] which promotes a pro-inflammatory state[30] also in the aging brain.[31,32] Coincidently, key molecules, risk factors, and physiological processes implicated in the pathogenesis of AD including Aβ assemblies,[33] tau aggregates within and beyond neurofibrillary changes,[34–37] apolipoprotein E (ApoE),[38,39] TREM2,[40–42] and the blood-brain barrier (BBB)[43,44] all interact with glial lineages, which mediate the pro-inflammatory state and contribute to synaptic failure including synaptophagy in AD brains.[19,45,46] The finding that systemic inflammatory signals correlate with cognitive decline[47,48] and regularly communicate and shape epigenetic programs of the glia in the brain[49] suggests that pro-inflammatory changes in AD brains can be set off also by peripheral causes. Considering ChP coordinates the crosstalk of the immune signals between the periphery and the brain,[22,50–56] these reports suggest that ChP dysfunction could contribute to the inflammatory state of AD brains.

The ChP Is a grape-like structure composed of a tight-junction-bound epithelium and the underlying stroma rich in fenestrated capillaries of peripheral vascular origin. This specific architecture creates a barrier between the peripheral blood and the cerebrospinal fluid (CSF), which circulates between the ventricles and the surface of the brain.[21,57,58] Through production of the CSF, ChP monitors and adjusts brain homeostasis[39] including the activation status of the brain immune system,[20,53] proliferation of neural stem cells[59] and cognitive behavior.[50,60,61] Aging results in profound structural and functional changes of the ChP in animals[22,50] and humans[62–64] alike with ChP for unknown reasons becoming significantly increased in volume.[65] Changes in the ChP have been extensively described also in animal models of AD,[52,61,66–68] while strikingly few studies to date examine ChP in patients with AD. These studies show altered structural integrity,[64] describe transcriptomic and proteomic profiles indicative of inflammatory changes and impaired metabolism,[62,67,69] and report preliminary correlations between ChP volumes, cognition, and biomarkers of AD.[70,71] Studies of the CSF also reveal extensive abnormalities including inflammatory changes in the CSF in aging[72–74] and AD[74–81] and further support the role of ChP in AD. The basis for these abnormalities is largely unknown. To address these gaps in our knowledge and to critically test for the involvement of the ChP in AD, we performed a series of pilot experiments to tease apart the effects of aging *versus* AD in the CSF and then systematically examine the structure of ChP in patients with AD.

1.2 | Study design and main results

We here ask what changes in the CSF environment surround ChP, systematically test for structural, inflammatory and metabolic changes of the *post-mortem* ChP and last investigate ChP in vivo in patients with AD. To answer these questions comprehensively, we use a diverse inventory of data sets and samples from different sources and cohorts.

RESEARCH IN CONTEXT

1. Systematic Review: The authors reviewed literature in PubMed using the terms "cerebrospinal fluid", "choroid plexus", "aging" and "Alzheimer's disease". In contrast to the cerebrospinal fluid (CSF), where changes during aging and in Alzheimer's disease (AD) are extensively reported, strikingly little is known about the role of the choroid plexus (ChP). Although severed structural integrity, transcriptomic and proteomic profiles and preliminary correlations between cognition, AD biomarkers, and ChP volumes were reported earlier, a systematic analysis of molecular changes in the ChP associated with AD is currently lacking.
2. Interpretation: Our study reveals a relationship between aging and AD in that changes in the CSF associated with aging are perturbed in the instance of AD. These CSF changes are associated with significant remodeling of the ChP in patients with AD, which in turn correlates with cognitive performance and reflects inflammatory signals and aberrant protein accumulations. Considering the ChP plays a critical role in brain homeostasis, this and previous studies provide mounting evidence of its dysfunction and participation in the pathogenesis of AD.
3. Future Directions: To clarify the role of the ChP in AD it is imperative to research: (1) the cause(s) of the observed ChP pathology in aged and AD brains, (2) the clinically relevant defects in brain homeostasis produced by dysfunctional ChP, and (3) the potential for a therapeutic strategy that normalizes ChP function in the instance of aging and AD.

To investigate changes in the CSF environment surrounding ChP in AD vis-à-vis natural aging, we analyzed a large publicly available data set of CSF proteomes consisting of healthy individuals and patients with AD[82,83] from scratch to take into account the effects of aging. To establish how specific are the CSF changes to AD, we used mass spectrometry to measure CSF proteins in patients with mild cognitive impairment (MCI) or dementia due to AD, an infectious neurological disease, acute Lyme polyradiculoneuritis (ALymeP), and a faster progressing neurodegenerative disorder, amyotrophic lateral sclerosis (ALS).

To test for structural, inflammatory and metabolic changes of the ChP *post mortem* in AD, we harvested ChP from the lateral cerebral ventricles including ChP from the temporal horns of healthy individuals and patients afflicted by AD and other neurological conditions. The formalin fixed paraffin embedded (FFPE) sections of ChP were stained with hematoxylin and eosin (H&E) to examine gross structural changes. To probe for neurodegenerative changes, the ChP were stained with markers for amyloid deposits, neurofibrillary changes and α-synuclein.

To test for inflammation, the FFPE sections were stained with markers for macrophages and T lymphocytes. RNA isolated from snap frozen ChP was evaluated by real-time polymerase chain reaction (RT-PCR) for the expression levels of different markers of immune system activation and lysates from snap frozen ChP were prepared to measure cytokine levels by ELISArray and western blots. To test for metabolic changes in the ChP, the same lysates used to measure cytokine levels were subject to mass spectrometry to quantify a number of CSF resident proteins selected using a random number table in addition to quantifying cholesterol and different lipids.

To investigate ChP in vivo, we first used a 1.5T magnetic resonance imaging (MRI) scanner to establish the intensities, structural changes and volumes of ChP in healthy individuals and patients with AD. Volumes of ChP were measured from three-dimensional (3D) reconstructions as well as manually from a randomly selected subset of originally acquired MRI brain images. A 3.0T MRI scanner was then used to measure ChP volumes at a higher resolution in an independent cohort of healthy individuals and AD patients to further validate our original findings. The ChP volumes were lastly correlated with age and the cognitive performance using the Mini-Mental State Examination (MMSE).

The abnormalities observed in the CSF of patients with AD consisted largely of aberrancies in the same biological processes that changed most significantly with aging in healthy individuals. These findings were most pronounced in the 66- to 75-year-old age group and suggest that ChP in AD is perpetually bathed in CSF exhibiting protein abnormalities that evolve with aging. The H&E stained FFPE sections of ChP showed age-related structural changes, which were indistinguishable between healthy individuals and patients afflicted by AD and other conditions at a light microscopy level. In AD, ChP exhibited significantly increased levels of several cytokines, aberrant accumulation of transthyretin (TTR) and Niemann-Pick intracellular cholesterol transporter 2 (NPC2) and reduced levels of GM1 ganglioside. Therefore, the ChP hosts unexpected inflammatory signals and aberrant accumulation of molecules involved in metabolic pathways in AD. Imaging showed significantly increased intensities and remodeling of ChP in AD patients. ChP volumes measured automatically, using 3D reconstructions, manually or with a 3.0T MRI scanner on a separate cohort were significantly increased in AD patients compared with healthy individuals. The ChP volumes correlated with age and inversely with cognitive performance in AD patients in vivo and thus provided clinical relevance to our *post-mortem* ChP findings in AD.

1.3 | Discussion and study conclusions

The preliminary experiments described here document an unexpected confluence of inflammatory signals and aberrant accumulation of metabolically active ChP resident proteins that are physiologically secreted into the CSF in patients with AD. Additionally, proteomic alterations including evidence of inflammation develop and perturb physiological process of aging in the CSF.[84] These findings are clinically relevant considering patients with AD show structural changes of the ChP, which correlate with aging and cognition.[84] Although these findings require further validation, they reveal a repertoire of ChP pathologies that lay the foundation for testing the role of ChP dysfunction mechanistically in the pathogenesis of AD.

In contrast to previous studies of the CSF in aging[72,85] and AD,[76,77,79,82,86] our analyses reveal that the same biological processes change in both of these conditions but to a different extent. This suggests that CSF changes in AD reflect a perturbed process of physiological aging. Changes in the inflammatory pathways identified in AD are more pronounced in other disorders we examined, possibly due to faster clinical progression of both AlymeP and ALS. Despite similarities, deeper analyses disclose subtle differences in inflammatory pathways between AD, AlymeP disease, and ALS,[87–89] which indicate an additional layer of inflammatory changes beyond aging. The finding that the most significant CSF changes in sporadic AD occur at the same time when the risk of AD starts increasing[90] raises the question of whether these changes relate causally to the pathogenesis, reflect brain pathology, or indicate a protective response.[77,91,92] The observations that CSF in the young exhibits restorative properties[93] and that a dampened immune response evolutionarily favors longevity,[94] support the notion that CSF changes in AD reflect pathological rather than physiological events.

The described abnormalities of the ChP validate and extend previously reported findings in animal models[67,68] and patients with AD,[64,69,95] which together with this study provide compelling evidence of ChP dysfunction in AD. Considering ChP provides the brain with nutrients and removes its waste, any dysfunction is expected to significantly perturb brain homeostasis.[21,58,96] This is further corroborated by the impaired production and altered composition of the CSF in aging[97] and in AD [85,98,99,100] Intriguingly, many of the cytokines that we found to increase in the ChP were previously reported having increased concentrations in the CSF in AD.[77,101] A lack of inflammatory infiltrates in the ChP suggests that these cytokines originate from the CSF, but could also be locally produced or reflect unresolved inflammation.[102] In all cases, functional ChP is essential for timely sensing and transmission of information about peripheral inflammatory insults to the brain.[52–56,61,103–105] It is improbable that dysfunctional ChP, bathed in a CSF marked by inflammatory changes,[84] senses and transmits such information to the brain in AD correctly. Therefore, the ChP in AD likely misconstrues the peripheral inflammatory status and contributes to the pro-inflammatory state of the brain beyond normal aging,[31,32,106–108] which promotes synaptic failure, impairs brain connectivity, reduces cognitive reserve, and ultimately culminates in cognitive decline.

We identify structural changes of the ChP in vivo in patients with AD, which correlate with aging and inversely with cognitive performance. Our findings are consistent with previously reported associations between ChP volumes, biomarkers of AD and cognition.[70,71] They extend previously noted association between aging[65] and ChP by showing that increased ChP volumes with aging undergo further increase and significant remodeling of their shapes in AD. Considering the paucity of in vivo studies of the ChP, it is essential to discern the diagnostic value of ChP changes in AD defined with biomarkers,[109]

post-mortem[110] or syndromically,[13] and relative to other dementias. Given the lack of efficient treatments for AD, our work suggests that strategies targeting ChP may be a novel and promising therapeutic option in the instance of AD and other neurodegenerative disorders.[111,112]

1.4 | Limitations, unanswered questions, and future directions

Although the use of *post-mortem* ChP tissue is critical to document human pathology, it comes with several shortcomings. Such tissues cannot provide mechanistic insights and are inevitably subject to a degree of damage caused by delayed collection. To circumvent the latter, we performed MRI imaging studies in patients with AD. Considering this was a pilot study, the results await further validation using larger sample sizes, different cohorts, and optimally longitudinal study design.

Despite the repertoire of ChP pathologies described in AD, the mechanisms underlying ChP damage in the pathogenesis of AD remain unclear. Considering ChP is bathed in the CSF, which is significantly altered in AD, a direct role of the CSF compromising ChP provides the simplest explanation. However, the fact that aging is the major risk factor for AD and simultaneously affects ChP and CSF suggests that inherent changes of the ChP beyond normal aging per se could also be at play. It remains in fact unknown whether upregulation of the host-defense programs[113] occurs properly during aging with enhanced AD risk. Although current studies suggest that increased ChP volumes observed by us and others[70,71] in AD are not the result of compensatory increase in the CSF production,[69,98,99] but rather of perturbed local blood flow and permeability,[114,115] significant further work is needed to provide a mechanistic account of the observed structural changes, the effects of systemic arterial hypertension,[116] and correlations with aging and cognitive performance.

Regardless of the mechanisms underlying ChP pathology in AD, the inflammatory, metabolic, and other changes of the ChP and the CSF suggest their contribution in perturbing brain homeostasis including the correct sensing and transmission of immune signals from the periphery to the brain[22,50] and call for studies of the role of the ChP in the pathogenesis of AD. Regrettably, current lack of bona fide cell and animal models of sporadic AD makes it extremely difficult to study mechanisms underlying ChP pathology and its repercussions. Testing how AD-like composition of the CSF alters ChP, investigating the effects of risk factors of AD on the structure and function of ChP and recapitulating aging and mimicking AD in ChP organoids[117] will likely open new vistas in our understanding of the ChP. A more nuanced understanding of transcytosis-mediated relays across the ChP in AD is also needed. Studying ChP longitudinally in patients afflicted by a range of neurodegenerative disorders, correlating its changes with behavior, cognition, and other neurological deficits, evaluating rigorously the effects of cardiovascular and other risk factors, and teasing apart the effects of compromised ChP from the disrupted BBB in AD[118,119] should be informative.

2 | CONSOLIDATED RESULTS AND STUDY DESIGN

To distinguish alterations of the CSF that can compromise ChP in AD from the effects of aging, we first re-examined a publicly available CSF proteomic data set representative of a wide age range of cognitively intact healthy individuals and patients with AD (Figure 1A). Half of the most significantly changed biological processes identified in the whole cohort consisted of pathways involving inflammation (Figure 1B). When the cohort was split to compare AD patients with healthy individuals, only innate immunity, neutrophil degranulation, complement cascade, and amyloid fiber formation related biological processes ranked higher in significance in AD (Figure 1C). The most prominent changes in biological processes coincided with the age period with the highest incidence of AD and consisted of biological processes involved in the inflammatory response, the immune system, interleukin signaling, cytokine-mediated signaling, innate immune system and immune cell activation (Figure 1E and F). Further mass spectrometry analyses revealed that the same biological processes were altered also in inflammatory and other neurodegenerative disorders of the brain (Figure 2A-C). However, in these disorders, different proteins underlay further exacerbated inflammatory pathways compared with AD (Figure 2D).

To test whether CSF abnormalities in AD are accompanied by compromised ChP, the ChP were harvested from lateral cerebral ventricles including their temporal horns and examined for their gross structure. Light microscopy of H&E stained FFPE sections of ChP showed similar degree of epithelial atrophy, stromal fibrosis, blood vessel thickening, and calcifications in healthy individuals and patients with AD (Figure 3A and B, Figure S1A-D). Furthermore, examination of the neuropathological hallmarks of neurodegeneration found no amyloid deposits, neurofibrillary changes, nor α-synuclein inclusions in the ChP of healthy individuals and patients afflicted by early or late AD or AD with Parkinson's disease (PD) (Figure S1E-T). To examine inflammatory changes, the ChP were evaluated for inflammatory infiltrates, activation of the immune cells and the cytokine levels. H&E stained ChP showed similar number of inflammatory cells in healthy individuals and patients afflicted by AD (Figure 3C). This finding was further confirmed by staining FFPE ChP sections with an anti-CD68 antibody, a bona fide marker of macrophages (Figure 3D). Since lack of inflammatory infiltrates does not inform about the activation of the immune cells in the ChP, we next examined the expression levels of different markers of the immune system activation by RT-PCR. There were no differences in the expression levels of different markers of the activation receptors, cytokines, immune cell activation, as well as of the T-cell activation between healthy individuals and patients with AD (Figure 3E). We last measured cytokines in lysates prepared from snap frozen ChP and found significantly increased levels in several pro- and anti-inflammatory cytokines in AD patients compared with healthy individuals (Figure 3F, Figure S2).

To investigate ChP in AD further, we measured the concentrations of a subset of randomly selected CSF proteins as a proxy measure

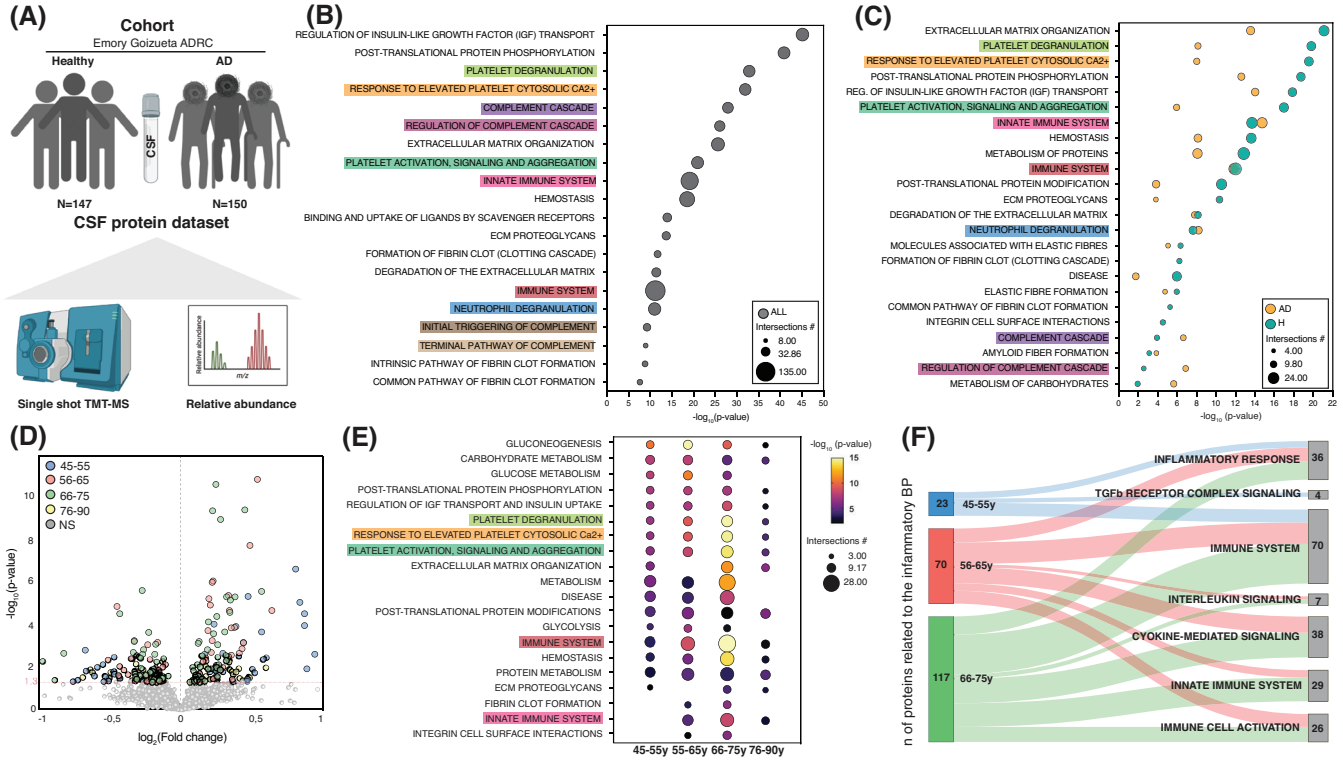

FIGURE 1 CSF in aging and AD. (A) Characteristics of the CSF protein database from the Emory Goizueta ADRC cohort. (B) The most significant Ingenuity pathways based on the CSF proteins changed by aging ($p \leq 0.05$). (C) The most significant Ingenuity pathways based on the CSF proteins changed by aging in healthy individuals *versus* AD ($p \leq 0.05$). (D) Volcano plot showing significantly changed CSF proteins in AD compared with healthy individuals in 45–55 ($n = 29$), 56–65 ($n = 97$), 66–75 ($n = 133$) and 76–90 ($n = 38$) year-old age groups ($p \leq 0.05$, NS: not significant). (E) The most significant Ingenuity pathways based on the CSF proteins changed by aging in AD compared with healthy individuals in different age groups ($p \leq 0.05$). (F) Sankey diagram showing significantly changed inflammatory pathways in AD compared with healthy individuals across different age groups ($p \leq 0.05$)

of its function. The proteotypic sequence of half of the randomly selected CSF proteins was successfully validated using isotopically labeled standards and their concentrations in the ChP measured using mass spectrometry (Figure 4A). In contrast to other proteins, NPC2 and TTR showed significantly increased levels in the ChP in patients with AD compared with healthy individuals. To investigate these protein changes further, we stained FFPE ChP sections with antibodies against NPC2 and TTR. We observed significantly increased mean intensities of both NPC2 and TTR in the ChP in AD patients compared with healthy individuals, predominantly located in the epithelium (Figure 4B and C). While both proteins have been previously associated with AD,[120,121] genetic dosage of NPC2 has also been reported to regulate cholesterol and lipid metabolism.[122] Mass spectrometry measurements showed significantly decreased levels of anti-inflammatory GM1 ganglioside, but not of cholesterol nor of other lipids in the ChP of patients with AD compared with healthy subjects (Figure 4D, Figures S3 and S4A-F).

To test whether changes identified in the ChP *post mortem* have a clinical or in vivo correlate in AD, we studied ChP using 1.5T MRI (Figure 5A). The T1 weighted sequences of ChP showed significantly increased intensities in AD patients compared with healthy individuals, which suggests that ChP undergoes changes in its composition in the course of AD (Figure 5B). Examination of the shapes of 3D reconstructed representations of the ChP is consistent with significant remodeling in AD considering the overall hypertrophy of the ChP accompanied by its atrophy along the anterior margins extending distally toward hippocampi (Figure 5C). Automated volumetric measurements of hippocampi, cerebellar cortices and ChP found significantly reduced volumes of the hippocampi, no changes in cerebellar cortices and significantly increased volumes of ChP in patients with AD (Figures 5D and 5E). To confirm this finding, volumes of 3D reconstructed representations were also measured and showed significantly reduced hippocampal and increased ChP volumes in AD patients (Figure 5F). ChP volumes are in this case smaller, because 3D representations are based on continuous triangulated surfaces and thus more accurate compared with the automated measurements, which are vulnerable to include also artefactual voxels. Manual measurements of ChP in a randomly selected subset of MRI brain images further confirmed this finding (Figure 5G). We last imaged ChP at a higher resolution using a 3T MRI and again reproduced previously observed increased ChP volumes in AD patients compared with healthy individuals in a separate cohort (Figure 5H). Notably, increased ChP volumes correlated with age and inversely with cognitive performance in patients with AD (Figure 5I and 5J).

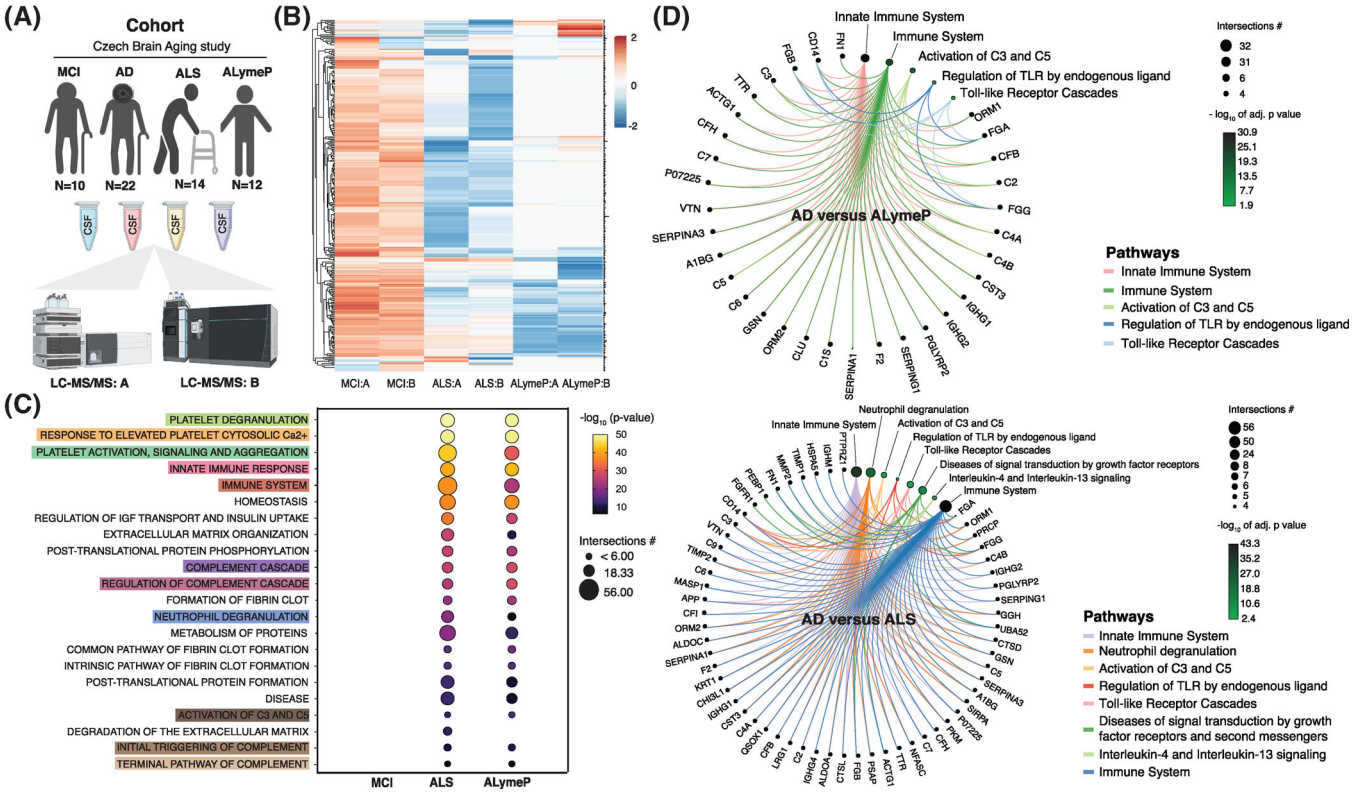

FIGURE 2 CSF in AD and other conditions (A) Characteristics of the Czech Brain Aging Study cohort.(B) Heatmap representing hierarchically clustered CSF proteins identified by two independent mass spectrometers and protocols (A and B) in MCI, ALymeP, and ALS compared with AD ($p \leq 0.05$ FDR adjusted t-test). (C) The most common significantly changed Reactome pathways in MCI, ALymeP, and ALS compared with AD ($p \leq 0.05$). (D) Circular netplots showing significantly changed inflammatory CSF proteins and pathways in AD compared with ALymeP and ALS ($p \leq 0.05$)

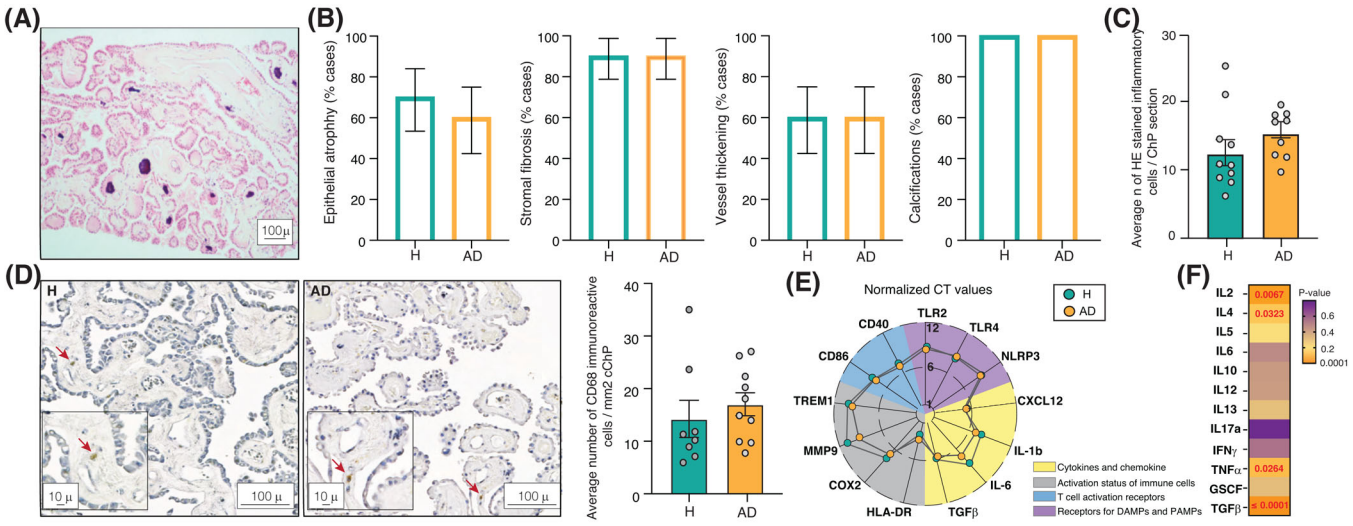

FIGURE 3 Structure and the inflammatory status of the ChP in AD. (A) Representative H&E stained FFPE section of the ChP. (B) Percentage of healthy individuals and AD patients showing epithelial atrophy, stromal fibrosis, vessel thickening and calcifications in the ChP. One technical replicate ± SEM; two-sample *t*-test ($p \leq 0.05$). (C) Average number of inflammatory cells in H&E stained ChP from healthy individuals and AD patients. Mean number of cells per six high-power microscopy fields per section ± SEM; two-sample *t*-test ($p \leq 0.05$). (D) Anti-CD68 antibody labelled cells in the ChP of healthy individuals and AD patients. Mean number of cells per 10 high-power microscopy fields per section ± S.E.M.; two-sample *t*-test ($p \leq 0.05$). (E) Expression levels of markers of the activation of the ChP immune cells in healthy individuals and AD. The lines crossing central, middle and outermost circle represent distances corresponding to normalized CT values of 1, 6, and 12, respectively. (F) ELISArray measured ChP cytokine levels in healthy individuals and AD. Mean of 3 technical replicates per sample ± SEM; two-sample *t*-test ($p \leq 0.05$)

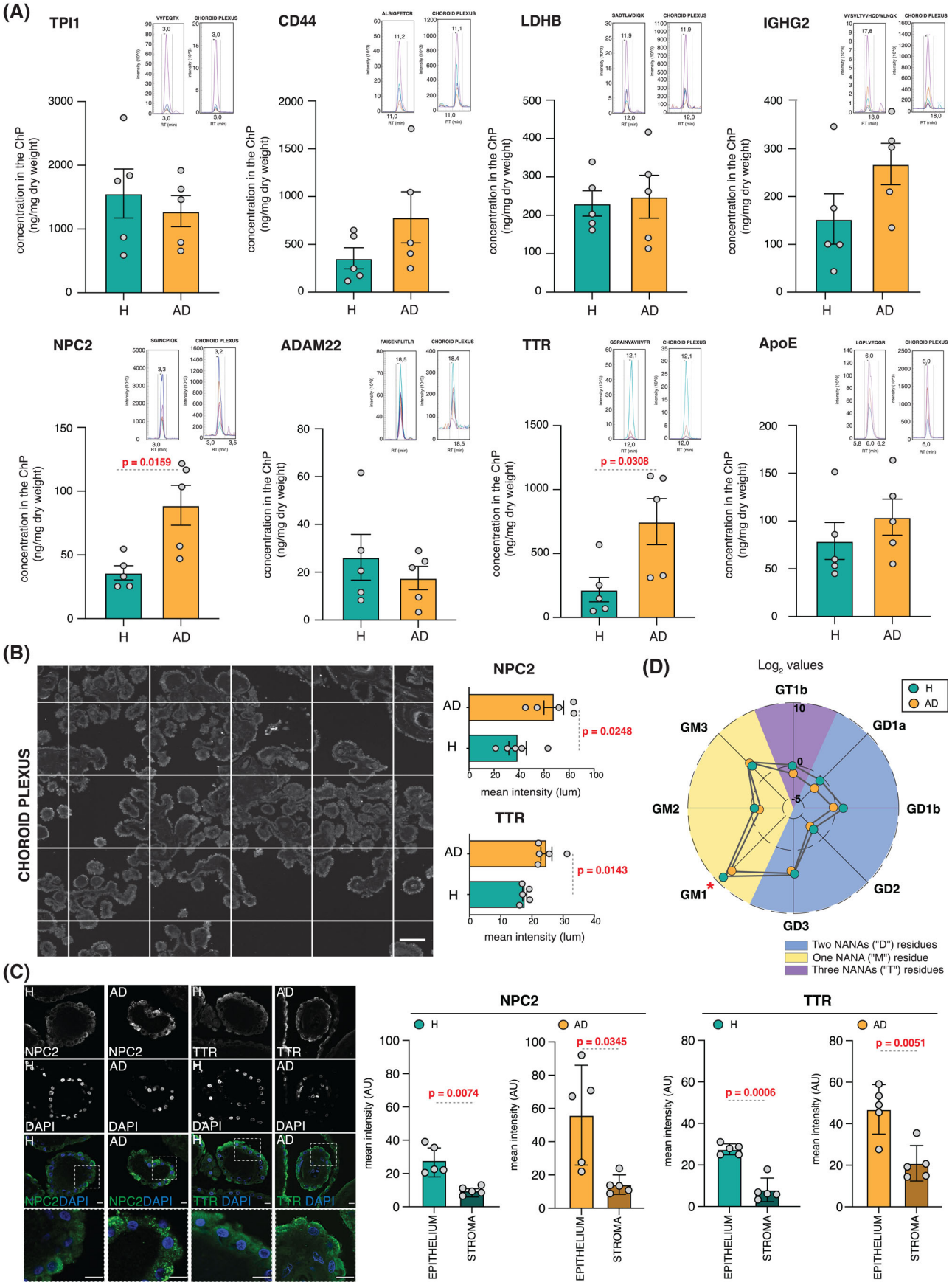

FIGURE 4 Aberrant accumulation of CSF resident proteins in the ChP in AD. (A) Levels of CSF resident proteins in the ChP of healthy individuals and AD patients. Skyline iRT retention time prediction algorithm showing identical chromatogram retention times between

3 | DETAILED METHODS AND RESULTS

3.1 | DETAILED METHODS

3.1.1 | Study participants

Clinical data and samples were obtained from the Emory Goizueta ADRC CSF proteomics of 300 individuals,[82,83] UCSD Shiley-Marcos ADRC, the Czech Brain Aging Study,[123] the Argentina ADNI,[124] the Barrow Neurological Institute[125] and the Imperial College Parkinson's UK Brain Bank[126] (Table S1). Collection of all samples was approved by the Institutional Review Boards of each participating institution with written consent obtained from all the individuals.

3.1.2 | Tissue collection

CSF samples were collected and stored following best practice protocols set forth by the National Institutes of Health Alzheimer's Disease Research Centers (NIH ADRCs) and others[123,125–128].

3.1.3 | Cognitive testing

All study individuals underwent comprehensive diagnostics consisting of clinical evaluation including laboratory tests and brain imaging according to NIH and other best practice guidelines.[123,125] ALymeP was diagnosed when individuals demonstrated clinical characteristics, increased CSF leukocyte count and positive serology for *Borrelia burgdorferi*.

3.1.4 | Pathology

Senile plaques were probed using the primary antibody recognizing amyloid-β (4G8, Covance), neurofibrillary changes using an antibody against phosphorylated tau (AT8, Thermo Fisher Scientific), and Lewy pathology using the α-synuclein clone 42 antibody (#610787, BD Transduction Labs).

3.1.5 | ELISArray

ChP were homogenized using a Bullet Blender (Next Advance). Samples were assessed for their protein content using Pierce BCA protein assay (Thermo Fisher Scientific). Cytokines were measured using Multi-Analyte ELISArray (QIAGEN). Cytokine levels were determined based on the absorbance values of negative (buffer) and positive (standards for all cytokines examined) controls. All measurements were normalized to the total protein content.

3.1.6 | Western blots

Protein lysates were separated on 4%–20% sodium dodecyl sulfate (SDS)-polyacrylamide gels and transferred to polyvinylidene fluoride (PVDF) membranes (Bio-Rad Laboratories). After blocking, membranes were incubated with antibodies against interleukin 2 (IL-2; D7A5, Cell Signaling Technology), IL-6 (#6672, Abcam), IL-10 (#34843, Abcam), tumor necrosis factor α (TNFα; #9739, Abcam), and transforming growth factor beta (TGFβ1; #3711, Cell Signaling Technology). Cytokine levels were normalized to β-actin.

3.1.7 | Immunohistochemistry

The PPFE ChP sections were blocked and incubated overnight with primary antibodies against NPC2 (1:50, sc-166449, Santa Cruz), TTR (1:500, A0002, DAKO), CD3 (1:500, NCL-LCD3-565, Novocastra), or CD68 (1:100, ab955, Abcam).

3.1.8 | Gene expression analysis

RNA was prepared using the miRNeasy kit (Qiagen, Germany) and transcribed using the High-Capacity cDNA Reverse Transcription Kit (Thermo Fisher Scientific). Quantitative RT-PCR (qPCR) was carried out with Taqman probes (Taqman Gene Expression Assay, Thermo Fisher Scientific) using TaqMan Gene Expression Master Mix (Thermo Fisher Scientific). qPCR analysis was performed using a LightCycler II (Roche). The Ct values (ΔCt) of genes of interest were normalized to house-keeping genes.

3.1.9 | Microscopy and image processing

ChP images were acquired at 10× using AxioScan.Z1 scanner microscope (Zeiss). Acquired images were analyzed using the Image Pro Premier 3D software (Media Cybernetics). Distribution of NPC2 and TTR was examined using a 63× oil-immersion objective with a confocal laser scanning microscope (Zeiss).

proteotypic peptides used to quantify ChP proteins (right) and stable isotopically labeled synthetic peptides (left). Mean of six technical replicates per sample ± S.E.M.; two-sample *t*-test ($p \leq 0.05$). (B) Mean intensities of NPC2 and TTR in the scanned ChP of heathy individuals and AD patients (magnification bar 100 μ). Mean of 90 technical replicates per sample ± S.E.M.; two-sample *t*-test ($p \leq 0.05$). (C) Mean NPC2 and TTR intensities in the confocal images of the ChP epithelium and stroma in healthy individuals and AD (magnification bar 10 μ). Mean of 3-12 technical replicates ± SEM; repeated measures ($p \leq 0.05$). (D) Levels of ChP gangliosides in healthy individuals and AD. Mean of six technical replicates per sample ± SEM; two-sample *t*-test ($p \leq 0.05$)

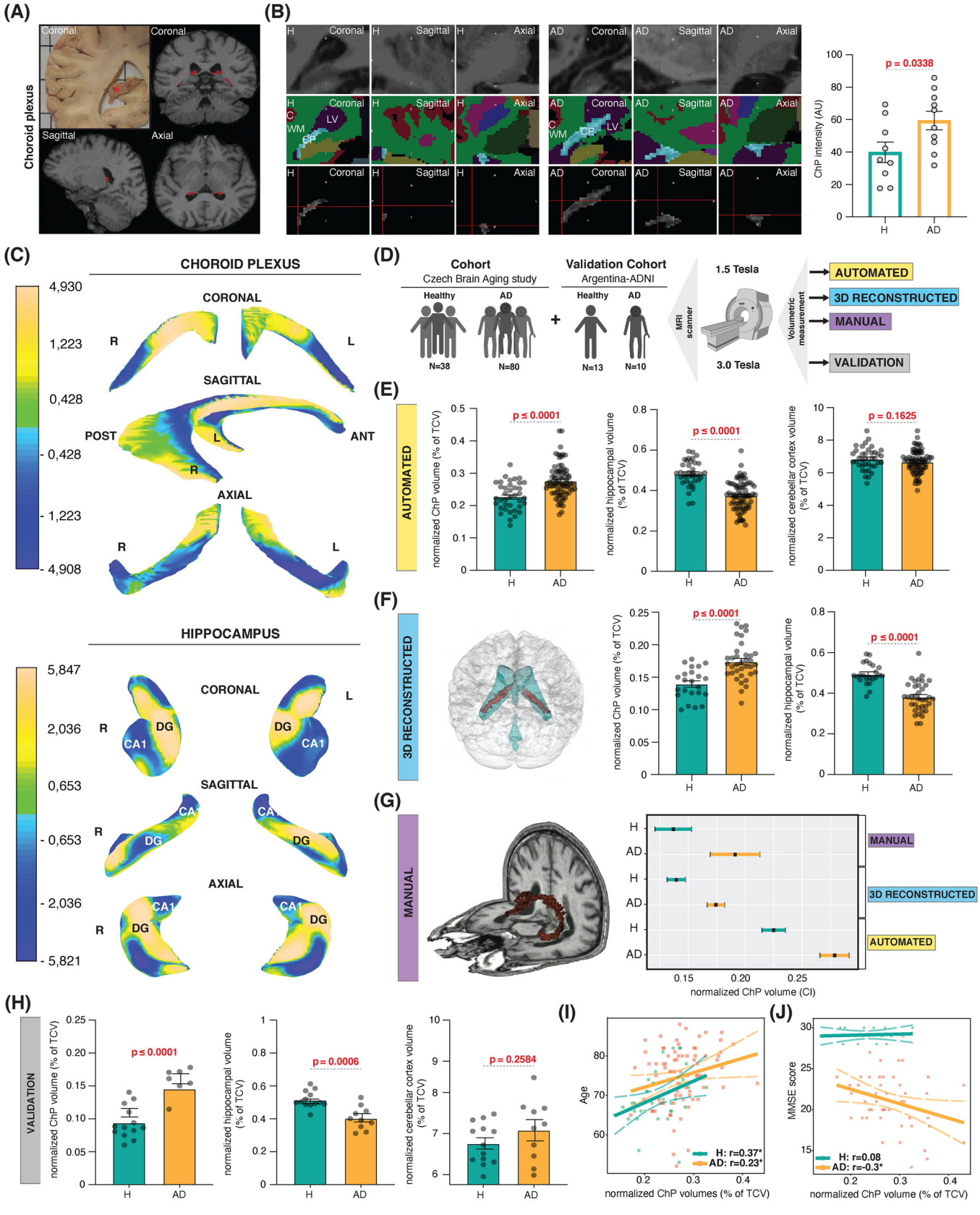

FIGURE 5 Increased intensity, remodeling, and volume of ChP in AD. (A) A coronal view of *post-mortem* ChP in the right lateral ventricles (red asterisk) and T1-weighted sequence derived positions of ChP in coronal, sagittal and axial views (in red). (B) Coronal, sagittal, and axial views of ChP representative of healthy individuals and AD patients visualized using T1-weighted sequence (top), FreeSurfer brain structure map (middle), and following ChP segmentation (bottom). Normalized ChP intensities in healthy individuals and AD. Individual measurements ± SEM; two-sample

3.1.10 | Quantitative histology

Six high-magnification ChP images per section stained with either H&E or the anti-CD-68 antibody were scored for the number of inflammatory cells. To measure total mean NPC2 and TTR intensities, a grid of 500 × 500 pixel squares was placed over each image. A total of 30 grid squares were randomly selected to sample intensities across the entire ChP. Three rectangular regions of interest per each grid square were examined for a total of 90 regions of interest per image. Mean intensities were calculated using Image Pro Premier 3D software (Media Cybernetics). To examine the distribution of NPC2 and TTR within the ChP, the sections were imaged with a 63× oil-immersion objective using a confocal laser scanning microscope (Zeiss). 1–4 ChP grape-like structures in three independent fields of view were sampled per each slide.

3.1.11 | Mass spectrometry proteomics of the CSF

CSF samples were analyzed using two independent mass spectrometry protocols. According to the first protocol (A), three technical replicates of 500 ng of tryptic peptides per sample were analyzed by LC-MS/MS using an UltiMate 3000 RSLCnano system (Thermo Fisher Scientific) coupled via an EASY-spray ion source (Thermo Fisher Scientific) to an Orbitrap Elite mass spectrometer (Thermo Fisher Scientific). According to the second protocol, one technical replicate of 1 μg of tryptic peptides per sample was analyzed by LC-MS/MS using an UltiMate 3000 RSLCnano system coupled to an Orbitrap Fusion Lumos tribrid mass spectrometer (both Thermo Fisher Scientific).

3.1.12 | CSF proteomic data processing

The raw data were analyzed using MaxQuant software (version 1.5.6.5). The MaxQuant output file (ProteinGroups.txt) was uploaded into Perseus software (version 1.6.1.1). Previously described 300 patient Emory cohort CSF tandem mass tag (TMT)-based quantitative discovery mode proteomics data set[82,83] was re-analyzed for age-stratified differences. In contrast to previous work, regression of age was not performed in the current analysis.

3.1.13 | Processing of ChP tissue for mass spectrometry assays and global lipid analysis

ChP samples were homogenized using BeadBlaster 24 (Benchmark Scientific Inc.). Isopropanol was added to each sample, which was vortexed, sonicated, and centrifuged at RT. The supernatant was then removed for the ganglioside and other assays (lipid extract). Remaining pellets were dried (Savant SDP121 P, SpeedVac, Thermo Fisher Scientific), reconstituted using glass beads in AmBic buffer with SDC, homogenized, vortexed and sonicated (protein extract). Synthetic isotopically labeled standard peptides containing an enzymatically cleavable tag at C-terminus were added to control for the variance in trypsin digestion.

3.1.14 | Validation of mass spectrometry targets

Gangliosides were quantified using selected reaction monitoring (SRM) assays in lipid extracts, which were internally standardized with isotopically labeled GM1 and GM3, respectively. Proteins were also analyzed using SRM assays for proteotypic peptides as protein surrogates. Tentative identifications of proteotypic peptides detected in ChP and concordant with the Skyline iRT Retention Time Prediction algorithm were validated using their isotopically-labeled analogs.

3.1.15 | Mass spectrometry quantitative protein assays

Dried solid-phase extracts of ChP digests were reconstituted in acetonitrile with formic acid. Samples were analyzed using ESI-UHPLC-SRM mass spectrometry on a triple quadrupole mass analyzer (1290 Infinity II and 6495B, Agilent) in positive ion detection mode.

3.1.16 | Mass spectrometry ganglioside assays

Gangliosides in lipid extracts of ChP were examined using both ESI-UHPLC-SRM positive and negative ion detection modes. Gangliosides were quantified with the stable isotope-labeled GM3 using appropriate response factors.

t-test ($p \leq 0.05$).(C) Mean changes in the shape of the 3D representations of the ChP and hippocampi in AD compared with healthy individuals. Single measurements ± SEM; two-sample *t*-test ($p \leq 0.05$). (D) Experimental design of the ChP volumetry study. (E) Automated measurements of normalized mean ChP, hippocampal and cerebellar cortical volumes in healthy individuals and AD. Individual measurements ± SEM; two-sample *t*-test ($p \leq 0.05$). (F) 3D reconstruction of the ChP (red) within the ventricular system (blue) in the brain. Normalized mean 3D representation-derived ChP and hippocampal volumes in healthy individuals and AD. Single measurements ± SEM; two-sample *t*-test ($p \leq 0.05$).(G) 3D representation of manually traced ChP (in red). 95% confidence intervals of normalized automated, 3D reconstructed and manually traced ChP volumes in healthy individuals and AD.(H) Normalized mean ChP, hippocampal and cerebellar cortical volumes in healthy individuals and AD. Individual measurements ± SEM; two-sample *t*-test ($p \leq 0.05$). (I) Correlation between normalized mean ChP volumes and age in healthy individuals and AD. Individual measurements ± SEM. (J) Correlation between normalized mean ChP volumes and MMSE scores in healthy individuals and AD. Individual measurements ± SEM.

3.1.17 | Mass spectrometry lipid analysis

Orbitrap Fusion (Thermo Fisher Scientific) and UHPLC (Nexera X2, LC-30AD, Shimadzu) with identical C18 column (Waters Corporation) thermostated at 40°C and gradient elution program as specified for ganglioside assays in the positive ion mode were used to measure lipids.

3.1.18 | Cholesterol spectrophotometric assay

Cholesterol was extracted from 1 mg of dry ChP tissue. The sample ultra-filtrate was transferred to a separate vial. Cholesterol was quantified using a colorimetric assay (MAK043, Sigma-Aldrich, USA).

3.1.19 | Brain MRI imaging

T1-weighted 3D high-resolution MRI images were acquired using magnetization-prepared rapid gradient echo (MP-RAGE) and fast spoiled gradient echo (FSPGR) pulse sequences using 1.5T (Siemens Avanto) in the Czech Brain Aging Study and 3.0T scanner (GE Signa HDxt) in the Argentina ADNI.

3.1.20 | MRI intensity measurements

Based on FreeSurfer wrapped in R, all segmented regions of interest and their masks were exported, including ChP intensities. Since raw intensities of ChP preclude their direct use in statistical analyses, we normalized raw intensity of ChP to CSF. The CSF strip algorithm was developed based on the white strip algorithm.[129]

3.1.21 | MRI volumetry measurements

Volumetric measurements were performed using FreeSurfer automated algorithm version v5.3 (http://surfer.nmr.mgh.harvard.edu/)[130–132] MRI images were further evaluated using 3D reconstructions. Automatic segmentation of FreeSurfer was used to obtain segmentation masks. To examine 3D differences in shape, ChP were represented with 4246 mesh points.

3.1.22 | Manual MRI tracing

Manual segmentation was performed on a slice per slice basis using Slicer (www.slicer.org) with a paintbrush of 0.5 mm. Once the region of interest was fully delineated, potential over- and under-segmented areas were checked in coronal orientation and segmentations corrected. 3D volume rendering was performed to test for appropriate spatial appearance of ChP in line with the expected anatomy.

3.1.23 | Statistical analysis

All statistical analyses were performed using commercially available softwares (R, Prism, SPSS, and SAS). CSF proteomic and brain imaging analyses were performed using R (v.4.1.0). RColorBrewer, igraph, ggraph, and ggplot2 packages were used for differential CSF protein expression analyses. Brain imaging analyses were performed using Whitestripe, FreeSurfer, NeuroBase, fslr, fsbrain, misc3d, rgl, and ggplot2.

3.2 | DETAILED RESULTS

3.2.1 | The effects of aging, AD, and other neurological disorders on the CSF

Since ChP is surrounded by the CSF, pathological CSF alterations can directly compromise its structure and function. To distinguish these alterations in AD from the effects of aging, the major risk factor of AD,[29] we investigated the relative abundance of CSF proteins in a well-established CSF proteomic data set of healthy individuals and patients with AD (Figure 1A)[82,83] Half of the most significantly changed biological processes overall consisted of inflammation-related pathways (Figure 1B). In contrast to healthy individuals, the majority of the most significantly changed biological processes by aging in AD showed reduced ranking in significance except for select pathways involved in inflammation and amyloid fiber formation (Figure 1C). Only pathways related to glucose, hyaluronan metabolism, binding and uptake of ligands by scavenger receptors were changed uniquely in AD patients. Our findings suggest that largely the same biological processes that change naturally with aging become perturbed in AD.

To investigate the relationship between aging, inflammation, and AD further, we divided the CSF proteomic cohort into four age groups (Figure 1D). The most pronounced changes between AD patients and healthy individuals occurred in the 66- to 75-year-old age group, which also showed the highest ranking in significance of the inflammatory pathways compared with all the other age groups (Figure 1E). Furthermore, the proteins and pathways involved in the inflammatory changes in the CSF of AD patients differed greatly between age groups (Figure 1F). These findings reveal an age-dependent evolution of proteins and pathways changing in the CSF of patients with AD compared with healthy individuals.

Studies of the CSF proteomic cohort provide compelling evidence that aging plays a role in the CSF changes in AD, but are not informative regarding their specificity to AD. To interrogate their specificity, CSF of patients with dementia due to AD were compared with CSF from patients with MCI, ALymeP, and ALS (Figure 2A). CSF samples were run on two separate mass spectrometers and only those CSF proteins that were identified by both approaches were used to build the CSF proteomes of individual disorders (Figure 2B). While there were expectedly no major differences in the CSF proteomes between MCI and AD, predominantly inflammatory pathways had higher

ranking in significance in patients with ALymeP and ALS compared with AD (Figure 2C). Patients with ALymeP and ALS also differed from AD in the proteins involved in the inflammatory pathways of CSF (Figure 2D). These findings suggest that biological processes undergoing changes in the CSF in AD are affected also by other neurological disorders with inflammatory and faster progressing neurodegenerative diseases showing more pronounced CSF changes.

3.2.2 | Structural, inflammatory, and metabolic changes of the ChP in AD

Inflammation invariably alters the structure and function of involved tissues.[84] Considering the intimate contact between ChP and CSF, the inflammatory CSF abnormalities suggest possible damage of the ChP structure in AD. To examine the structure of the ChP, FFPE sections harvested from lateral cerebral ventricles including samples from the temporal horns were stained with H&E (Figure 3A). Light microscopy revealed comparable degree of epithelial atrophy, stromal fibrosis, blood vessel thickening, and calcifications in the ChP of healthy individuals and AD patients (Figure 3B, Figure S1A-D). Staining for amyloid, neurofibrillary changes, and α-synuclein also demonstrated lack of hallmark lesions in the ChP of patients with early or late AD or AD with PD (Figure S1E-T). ChP, therefore, exhibit no overt structural changes nor pathology in AD.

Staining with H&E (Figure 3C) or with anti-CD68 and anti-CD3 antibodies (Figure 3D), which label macrophages and T lymphocytes, respectively, showed no evidence of inflammatory infiltrates in AD patients compared with healthy individuals. We next investigated the activation status of the ChP immune system by screening RNA from snap frozen ChP for the expression levels of the activation receptors, TLR4, TLR9, and NLRP3; cytokines, IL1β, IL6, and TGFβ; immune cell activation, TREM1, HLA-DR, COX2, and MMP9; and T-cell activation, CD40 and CD86 using RT-PCR. The expression levels of markers of the activation of the immune system were comparable between healthy individuals and AD patients (Figure 3E). We last measured cytokines in lysates from snap frozen ChP by an ELISArray. In contrast to healthy individuals, AD patients showed significantly increased levels of IL-2, IL-4, TNFα, and TGFβ in the ChP (Figure 3F). We separated lysates also by SDS-PAGE and confirmed significantly increased cytokine levels in the ChP of AD patients (Figure S2). ChP in AD, therefore, lack infiltration or activation of inflammatory cells, but display unexpected inflammatory signals.

To assess the function of the ChP in AD, we quantified CSF proteins in the ChP as a proxy measure of metabolic damage. Proteotypic sequences of 8 out of 16 randomly selected CSF resident proteins passed the validation and their ChP levels quantified using mass spectrometry (Figure 4A). Levels of NPC2 and TTR were significantly increased in the ChP of AD patients compared with healthy individuals. Scans of ChP stained with antibodies against NPC2 and TTR further corroborated this finding (Figure 4B), while confocal imaging showed that aberrant accumulation of NPC2 and TTR immunoreactivity in the ChP is confined predominantly to the epithelium (Figure 4C). Metabolically active proteins that are physiologically secreted from the ChP into the CSF, therefore, aberrantly accumulate in AD. Considering NPC2 deficiency perturbs lipid metabolism[122] and increases ganglioside levels,[121] we asked whether increased NPC2 levels show decreased ganglioside levels or otherwise perturbed lipid metabolism in the ChP in AD. Measurements of cholesterol, gangliosides, phosphatidylcholines, phosphatidylethanolamines, sphingomyelins, phosphatidylinositols, phosphatidylserines found reduced levels of GM1 ganglioside, but not of cholesterol nor of any other lipid specie in AD patients compared with healthy individuals (Figure 4D, Figure S3 and S4A-F). Considering GM1 harbors anti-inflammatory properties,[133] reduced GM1 levels further indicate perturbed inflammatory milieu of the ChP in AD.

3.2.3 | Imaging changes of ChP in AD patients

While our study provides evidence of compromised ChP in AD in *post-mortem* tissue samples, its clinical relevance remains to be established. To test this, we investigated structural changes of ChP in living healthy individuals and AD patients using MRI (Figure 5A). We first measured intensities of T1-weighted MRI images of ChP acquired using a 1.5T MRI scanner. Intensities of ChP were significantly increased in patients with AD compared to healthy individuals (Figure 5B). Considering this observation suggests remodeling of ChP in AD, we next examined changes in the shape of 3D reconstructed representations of the ChP and hippocampi. ChP exhibited significant overall hypertrophy with atrophic changes along the anterior margins extending distally toward the hippocampi in AD patients compared with healthy individuals (Figure 5C). Hippocampi showed previously described atrophic changes across their entire structure.[134] These experiments demonstrate that ChP undergoes significant structural changes in AD.

To test for changes in the size of the ChP, we next performed volumetric measurements of the ChP, hippocampi, which have been extensively reported to decrease in AD[135] and cerebellar cortices since previous reports found no major changes in AD[136] (Figure 5D). An automated volumetric measurement showed that ChP volumes significantly increased, while hippocampal volumes expectedly decreased and cerebellar cortices showed no changes in AD patients compared with healthy individuals (Figure 5E). To test this observation further, we measured volumes of 3D representations of ChP and hippocampi reconstructed from a randomly selected subset of MRI images. While 3D representations of hippocampal volumes demonstrated expected decrease, ChP volumes were significantly increased in AD patients (Figure 5F). To avoid segmentation-derived measurement errors,[137] we last measured ChP volumes manually. Manual measurements showed no overlap between the 95% confidence intervals of the ChP volumes in AD patients compared with healthy individuals further reinforcing the veracity of our findings (Figure 5G). We last acquired MRI brain images from a separate cohort using a 3.0T MRI scanner. In contrast to the hippocampal volumes, the ChP volumes were significantly increased in AD patients (Figure 5H). Increased ChP volumes

demonstrated stronger association with age in healthy individuals compared with AD patients (Figure 5I). AD patients, but not healthy individuals, also showed significant inverse correlation between ChP volumes and the MMSE scores (Figure 5J). Therefore, the larger the ChP volume, the poorer the cognitive performance in AD patients. Taken together, these experiments demonstrate the clinical relevance of our findings in regard to changes that we have noted *post mortem* in the ChP in AD.

AUTHOR CONTRIBUTIONS

Gorazd B. Stokin designed and planned the study, Maria Čarna and Gorazd B. Stokin analysed all of the data and wrote the manuscript, Isaac G. Onyango performed ChP cytokine experiments and analysis, Clara Limbäck-Stokin and Robert A. Rissman provided ChP samples, Clara Limbäck-Stokin performed all the ChP neuropathological experiments and analysis, Nadine Bakkar, Robert Bowser, Jakub Hort, and Kateřina Sheardova contributed CSF samples, Victoria David-Dirgo, Krystine Garcia-Mansfield, Dušan Holub, Ritin Sharma, and Patrick Pirrotte performed all the CSF mass spectrometry experiments, Jiři Damborsky, Durga Jha, Marketa Nezvedova, and Zdenek Spacil performed all the ChP mass spectrometry and other lipid experiments, Valentina Lacovich and Kateřina Texlova performed ChP immunohistochemistry and analysis, Hernan Chaves, Jakub Hort, Zuzana Nedelska, Lucia Pertierra Hana Markova, Gustavo Sevlever and Martin Vyhnalek were involved in the acquisition and analysis of MRI images, Stanislav Katina and Martin Vyhnalek performed MRI image and shape programming and analysis, including intensities and volumes, Ruben Houbrechts and Thijs Vande Vyvere performed manual ChP measurements, Maria Čarna, Eric B. Dammer, and Dušan Holub performed all the bioinformatics assessments and analysis, Silvie Belaškova, Jiři Damborsky, and Jan S. Novotny performed biostatistical analysis, Robert Bowser, Silvie Belaškova, Jiři Damborsky, Giancarlo Forte, Jan Frič, Jakub Hort, Patrick Pirrotte, Clara Limbäck-Stokin, Nicholas T. Seyfried, Gustavo Sevlever, Zdeněk Spačil, and Richard A. Smith provided continuous input during experiments and data analysis.

ACKNOWLEDGMENTS

Authors acknowledge Katja Klosterman and other members of the Stokin Lab, Michal Šitina and the Biostatistics core facility of the International Clinical Research Center of St. Anne's University Hospital, Kateřina Coufalikova from the RECETOX Centre of the Faculty of Sciences, Masaryk University, Kathleen Myers of the Center for Neurologic Study and Jeffrey Metcalf and Sara Shuldberg from the Rissman Lab. We are grateful to the participants, families, and all others involved in the Czech Brain Aging Study, Argentina Alzheimer's Disease Neuroimaging Initiative, Shiley-Marcos ADRC at the UCSD, Imperial College Parkinson's UK Brain Bank, Institute of Molecular and Translational Medicine, the ALS Tissue Bank and Target ALS Post-mortem Core, and Barrow Neurological Institute. We thank PrecisionMed for their guidance regarding human tissues. This study was supported by the European Regional Development Funds No. CZ.02.1.01/0.0/0.0/16_019/0000868 ENOCH grant (S.B., J.D., G.F., J.F., M.H., J.H., S.K. and G.B.S.), The EU Horizon 2020 research and innovation programme under grant agreement No. 857560 and CZ.02.1.01/0.0/0.0/17_043/0009632 CETOCOEN EXCELLENCE Teaming grant (J.D., G.B.S. and Z.S.), THE Cetocoen Plus grant CZ.02.1.01/0.0/0.0/15_003/0000469 (Z.S.), the Czech Ministry of Health grants NV 18–04–00346 (Z.N.), 18–04–00455 (J.H.), 00064203 (J.H.) and 19–08–00472 (Z.S. and K.S.), the Inbio grant No. CZ.02.1.01/0.0/0.0/16_026/0008451 (J.D.), the NIH grant P30 AGO62429 (R.A.R.), the Barrow Neurological Foundation and the Fein Foundation grant (R.B.), the research infrastructure LM2018121 RECETOX grant (Z.S.), the Grant Agency of the Masaryk University No. MUNI/G/1131/2017 GAMU grant (Z.S.), the National Cancer Institute of the NIH grant No. P30CA033572 (E.B.D. and N.T.S.), the NIA U01 grant U01AG061357 (E.B.D. and N.T.S.), the LX22NPO5107(MEYS) Next Generation EU grant (J.F) and the Institutional Support of Excellence 2.2 LF UK grant 6980382 (J.H.).

CONFLICTS OF INTEREST

The authors report no competing interests. Author disclosures are available in the supporting information.

REFERENCES

1. Cummings JL. Cognitive and behavioral heterogeneity in Alzheimer's disease: seeking the neurobiological basis. *Neurobiol Aging*. 2000;21:845-861. doi: 10.1016/s0197-4580(00)00183-4
2. Katzman R. Editorial: the prevalence and malignancy of Alzheimer disease. A major killer. *Arch Neurol*. 1976;33:217-221. doi: 10.1001/archneur.1976.00500040001001
3. Masliah E, Miller A, Terry RD. The synaptic organization of the neocortex in Alzheimer's disease. *Med Hypotheses*. 1993;41:334-340. doi: 10.1016/0306-9877(93)90078-5
4. Rodríguez-Arellano JJ, Parpura V, Zorec R, Verkhratsky A. Astrocytes in physiological aging and Alzheimer's disease. *Neuroscience*. 2016;323:170-182. doi: 10.1016/j.neuroscience.2015.01.007
5. Escartin C, Galea E, Lakatos A, et al. Reactive astrocyte nomenclature, definitions, and future directions. *Nat Neurosci*. 2021;24:312-325. doi: 10.1038/s41593-020-00783-4
6. Leng F, Edison P. Neuroinflammation and microglial activation in Alzheimer disease: where do we go from here? *Nat Rev Neurol*. 2021;17:157-172. doi: 10.1038/s41582-020-00435-y
7. Nieto-Sampedro M, Mora F. Active microglia, sick astroglia and Alzheimer type dementias. *Neuroreport*. 1994;5:375-380. doi: 10.1097/00001756-199401120-00001
8. Terry RD, Gonatas NK, Weiss M. Ultrastructural studies in Alzheimer's presenile dementia. *Am J Pathol*. 1964;44:269-297.
9. Braak H, Thal DR, Ghebremedhin E, Del Tredici K. Stages of the pathologic process in Alzheimer disease: age categories from 1 to 100 years. *J Neuropathol Exp Neurol*. 2011;70:960-969. doi: 10.1097/NEN.0b013e318232a379
10. Katzman R, Terry R, Deteresa R, et al. Clinical, pathological, and neurochemical changes in dementia: a subgroup with preserved mental status and numerous neocortical plaques. *Ann Neurol*. 1988;23:138-144. doi: 10.1002/ana.410230206
11. Kovacs GG. Tauopathies. *Handb Clin Neurol*. 2017;145:355-368. doi: 10.1016/B978-0-12-802395-2.00025-0
12. Jellinger KA. Recent update on the heterogeneity of the Alzheimer's disease spectrum. *J Neural Transm (Vienna)*. 2022;129:1-24. doi: 10.1007/s00702-021-02449-2
13. Breitner JCS, Dodge HH, Khachaturian ZS, Khachaturian AS. "Exceptions that prove the rule"—why have clinical trials failed to show efficacy of risk factor interventions suggested by observational

studies of the dementia-Alzheimer's disease syndrome? *Alzheimers Dement*. 2022;18:389-392. doi: 10.1002/alz.12633
14. Grady CL. Altered brain functional connectivity and impaired short-term memory in Alzheimer's disease. *Brain*. 2001;124:739-775. doi: 10.1093/brain/124.4.739
15. Sze C-I, Troncoso JC, Kawas C, Moution P, Price DL, Martin LJ. Loss of the presynaptic vesicle protein synaptophysin in hippocampus correlates with cognitive decline in Alzheimer disease. *J Neuropathol Exp Neurol*. 1997;56:933-944. doi: 10.1097/00005072-199708000-00011
16. Terry RD, Masliah E, Salmon DP, et al. Physical basis of cognitive alterations in Alzheimer's disease: synapse loss is the major correlate of cognitive impairment. *Ann Neurol*. 1991;30:572-580. doi: 10.1002/ana.410300410
17. Passamonti L, Tsvetanov KA, Jones PS, et al. Neuroinflammation and functional connectivity in Alzheimer's disease: interactive influences on cognitive performance. *J Neurosci*. 2019;39:7218-7226. doi: 10.1523/JNEUROSCI.2574-18.2019
18. Barthet G, Mulle C. Presynaptic failure in Alzheimer's disease. *Prog Neurobiol*. 2020;194:101801. doi: 10.1016/j.pneurobio.2020.101801
19. Hong S, Beja-Glasser VF, Nfonoyim BM, et al. Complement and microglia mediate early synapse loss in Alzheimer mouse models. *Science*. 2016;352:712-716. doi: 10.1126/science.aad8373
20. Schwartz M, Baruch K. The resolution of neuroinflammation in neurodegeneration: leukocyte recruitment via the choroid plexus. *EMBO J*. 2014;33:7-22. doi: 10.1002/embj.201386609
21. Ghersi-Egea J-F, Strazielle N, Catala M, Silva-Vargas V, Doetsch F, Engelhardt B. Molecular anatomy and functions of the choroidal blood-cerebrospinal fluid barrier in health and disease. *Acta Neuropathol*. 2018;135:337-361. doi: 10.1007/s00401-018-1807-1
22. Zhu L, Stein LR, Kim D, et al. Klotho controls the brain-immune system interface in the choroid plexus. *Proc Natl Acad Sci U S A*. 2018;115:E11388-E11396. doi: 10.1073/pnas.1808609115
23. Bertram L, Tanzi RE. The genetics of Alzheimer's disease. *Prog Mol Biol Transl Sci*. 2012;107:79-100. doi: 10.1016/B978-0-12-385883-2.00008-4
24. Masters CL, Selkoe DJ. Biochemistry of amyloid beta-protein and amyloid deposits in Alzheimer disease. *Cold Spring Harb Perspect Med*. 2012;2:a006262. doi: 10.1101/cshperspect.a006262
25. Selkoe DJ, Hardy J. The amyloid hypothesis of Alzheimer's disease at 25 years. *EMBO Mol Med*. 2016;8:595-608. doi: 10.15252/emmm.201606210
26. Kuller LH, Lopez OL. ENGAGE and EMERGE: truth and consequences? *Alzheimers Dement*. 2021;17:692-695. doi: 10.1002/alz.12286
27. Lie PPY, Yoo L, Goulbourne CN, et al. Axonal transport of late endosomes and amphisomes is selectively modulated by local Ca(2+) efflux and disrupted by PSEN1 loss of function. *Sci Adv*. 2022;8:eabj5716. doi: 10.1126/sciadv.abj5716
28. Stokin GB, Lillo C, Falzone TL, et al. Axonopathy and transport deficits early in the pathogenesis of Alzheimer's disease. *Science*. 2005;307:1282-2128. doi: 10.1126/science.1105681
29. Brookmeyer R, Evans DA, Hebert L, et al. National estimates of the prevalence of Alzheimer's disease in the United States. *Alzheimers Dement*. 2011;7:61-73. doi: 10.1016/j.jalz.2010.11.007
30. Gruver Al, Hudson LI, Sempowski GD. Immunosenescence of ageing. *J Pathol*. 2007;211:144-156. doi: 10.1002/path.2104
31. Lee C-K, Weindruch R, Prolla TA. Gene-expression profile of the ageing brain in mice. *Nat Genet*. 2000;25:294-297. doi: 10.1038/77046
32. Lu T, Pan Y, Kao S-Y, et al. Gene regulation and DNA damage in the ageing human brain. *Nature*. 2004;429:883-891. doi: 10.1038/nature02661
33. Soscia SJ, Kirby JE, Washicosky KJ, et al. The Alzheimer's disease-associated amyloid beta-protein is an antimicrobial peptide. *PLoS One*. 2010;5:e9505. doi: 10.1371/journal.pone.0009505
34. Jiang S, Maphis NM, Binder J, et al. Proteopathic tau primes and activates interleukin-1beta via myeloid-cell-specific MyD88- and NLRP3-ASC-inflammasome pathway. *Cell Rep*. 2021;36:109720. doi: 10.1016/j.celrep.2021.109720
35. Guo T, Noble W, Hanger DP. Roles of tau protein in health and disease. *Acta Neuropathol*. 2017;133:665-704. doi: 10.1007/s00401-017-1707-9
36. Terry RD. The fine structure of neurofibrillary tangles in Alzheimer's disease. *J Neuropathol Exp Neurol*. 1963;22:629-642. doi: 10.1097/00005072-196310000-00005
37. Kidd M. Paired helical filaments in electron microscopy of Alzheimer's disease. *Nature*. 1963;197:192-193. doi: 10.1038/197192b0
38. Machlovi SI, Neuner SM, Hemmer BM, et al. APOE4 confers transcriptomic and functional alterations to primary mouse microglia. *Neurobiol Dis*. 2022;164:105615. doi: 10.1016/j.nbd.2022.105615
39. Martens YA, Zhao N, Liu C-C, et al. ApoE cascade hypothesis in the pathogenesis of Alzheimer's disease and related dementias. *Neuron*. 2022;110:1304-1317. doi: 10.1016/j.neuron.2022.03.004
40. Sayed FA, Kodama L, Fan Li, et al. AD-linked R47H-TREM2 mutation induces disease-enhancing microglial states via AKT hyperactivation. *Sci Transl Med*. 2021;13:eabe3947. doi: 10.1126/scitranslmed.abe3947
41. Zhou Y, Song WM, Andhey PS, et al. Human and mouse single-nucleus transcriptomics reveal TREM2-dependent and TREM2-independent cellular responses in Alzheimer's disease. *Nat Med*. 2020;26:131-142. doi: 10.1038/s41591-019-0695-9
42. Jonsson T, Stefansson K. TREM2 and neurodegenerative disease. *N Engl J Med*. 2013;369:1568-1569. doi: 10.1056/NEJMc1306509
43. Sweeney MD, Ayyadurai S, Zlokovic BV. Pericytes of the neurovascular unit: key functions and signaling pathways. *Nat Neurosc i*. 2016;19:771-783. doi: 10.1038/nn.4288
44. Sweeney MD, Montagne A, Sagare AP, et al. Vascular dysfunction—the disregarded partner of Alzheimer's disease. *Alzheimers Dement*. 2019;15:158-167. doi: 10.1016/j.jalz.2018.07.222
45. Sekiya M, Wang M, Fujisaki N, et al. Integrated biology approach reveals molecular and pathological interactions among Alzheimer's Abeta42, Tau, TREM2, and TYROBP in Drosophila models. *Genome Med*. 2018;10:26. doi: 10.1186/s13073-018-0530-9
46. Sadick JS, O'dea MR, Hasel P, Dykstra T, Faustin A, Liddelow SA. Astrocytes and oligodendrocytes undergo subtype-specific transcriptional changes in Alzheimer's disease. *Neuron*. 2022;11:1788-1805. doi: 10.1016/j.neuron.2022.03.008
47. Darweesh SKL, Wolters FJ, Ikram MA, Wolf F, Bos D, Hofman A. Inflammatory markers and the risk of dementia and Alzheimer's disease: a meta-analysis. *Alzheimers Dement*. 2018;14:1450-1459. doi: 10.1016/j.jalz.2018.02.014
48. Holmes C, Cunningham C, Zotova E, Culliford D, Perry VH. Proinflammatory cytokines, sickness behavior, and Alzheimer disease. *Neurology*. 2011;77:212-218. doi: 10.1212/WNL.0b013e318225ae07
49. Wendeln A-C, Degenhardt K, Kaurani L, et al. Innate immune memory in the brain shapes neurological disease hallmarks. *Nature*. 2018;556:332-338. doi: 10.1038/s41586-018-0023-4
50. Baruch K, Deczkowska A, David E. Aging-induced type I interferon response at the choroid plexus negatively affects brain function. *Science*. 2014;346:89-93. doi: 10.1126/science.1252945
51. Baruch K, Ron-Harel N, Gal H, et al. CNS-specific immunity at the choroid plexus shifts toward destructive Th2 inflammation in brain aging. *Proc Natl Acad Sci U S A*. 2013;110:2264-2269. doi: 10.1073/pnas.1211270110
52. Baruch K, Rosenzweig N, Kertser A, et al. Breaking immune tolerance by targeting Foxp3(+) regulatory T cells mitigates

Alzheimer's disease pathology. *Nat Commun*. 2015;6:7967. doi: 10.1038/ncomms8967
53. Salvesen Ø, Reiten MR, Espenes A, Bakkebø MK, Tranulis MA, Ersdal C. LPS-induced systemic inflammation reveals an immunomodulatory role for the prion protein at the blood-brain interface. *J Neuroinflammation*. 2017;14:106. doi: 10.1186/s12974-017-0879-5
54. Strominger I, Elyahu Y, Berner O, et al. The choroid plexus functions as a niche for T-cell stimulation within the central nervous system. *Front Immunol*. 2018;9:1066. doi: 10.3389/fimmu.2018.01066
55. Yang AC, Kern F, Losada PM, et al. Dysregulation of brain and choroid plexus cell types in severe COVID-19. *Nature*. 2021;595:565-571. doi: 10.1038/s41586-021-03710-0
56. Balusu S, Van Wonterghem E, De Rycke R, et al. Identification of a novel mechanism of blood-brain communication during peripheral inflammation via choroid plexus-derived extracellular vesicles. *EMBO Mol Med*. 2016;8:1162-1183. doi: 10.15252/emmm.201606271
57. Cushing H. Studies on the cerebro-spinal fluid: I. Introduction. *J Med Res*. 1914;31:1-19.
58. Damkier HH, Brown PD, Praetorius J. Cerebrospinal fluid secretion by the choroid plexus. *Physiol Rev*. 2013;93:1847-1892. doi: 10.1152/physrev.00004.2013
59. Silva-Vargas V, Maldonado-Soto AR, Mizrak D, Codega P, Doetsch F. Age-dependent niche signals from the choroid plexus regulate adult neural stem cells. *Cell Stem Cell*. 2016;19:643-652. doi: 10.1016/j.stem.2016.06.013
60. Liu C-B, Wang R, Yi Y-F, Gao Z, Chen Yi-Z. Lycopene mitigates beta-amyloid induced inflammatory response and inhibits NF-kappaB signaling at the choroid plexus in early stages of Alzheimer's disease rats. *J Nutr Biochem*. 2018;53:66-71. doi: 10.1016/j.jnutbio.2017.10.014
61. Xu Z, Liu C, Wang R, Gao X, Hao C, Liu C. A combination of lycopene and human amniotic epithelial cells can ameliorate cognitive deficits and suppress neuroinflammatory signaling by choroid plexus in Alzheimer's disease rat. *J Nutr Biochem*. 2020;88:108558. doi: 10.1016/j.jnutbio.2020.108558
62. Pearson A, Ajoy R, Crynen G, et al. Molecular abnormalities in autopsied brain tissue from the inferior horn of the lateral ventricles of nonagenarians and Alzheimer disease patients. *BMC Neurol*. 2020;20:317. doi: 10.1186/s12883-020-01849-3
63. Tahira A, Marques F, Lisboa B, et al. Are the 50's, the transition decade, in choroid plexus aging? *Geroscience*. 2021;43:225-237. doi: 10.1007/s11357-021-00329-x
64. Serot J-M, Béné M-C, Foliguet B, Faure GC. Morphological alterations of the choroid plexus in late-onset Alzheimer's disease. *Acta Neuropathol*. 2000;99:105-108. doi: 10.1007/pl00007412
65. Alisch JSR, Kiely M, Triebswetter C, et al. Characterization of age-related differences in the human choroid plexus volume, microstructural integrity, and blood perfusion using multiparameter magnetic resonance imaging. *Front Aging Neurosci*. 2021;13:734992. doi: 10.3389/fnagi.2021.734992
66. GonzãLez-Marrero I, Gimenez-Llort L, Johanson CE, et al. Choroid plexus dysfunction impairs beta-amyloid clearance in a triple transgenic mouse model of Alzheimer's disease. *Front Cell Neurosci*. 2015;9:17. doi: 10.3389/fncel.2015.00017
67. Steeland S, Gorlé N, Vandendriessche C, et al. Counteracting the effects of TNF receptor-1 has therapeutic potential in Alzheimer's disease. *EMBO Mol Med*. 2018;10:8300. doi: 10.15252/emmm.201708300
68. Brkic M, Balusu S, Van Wonterghem E, et al. Amyloid beta oligomers disrupt blood-CSF barrier integrity by activating matrix metalloproteinases. *J Neurosci*. 2015;35:12766-12778. doi: 10.1523/JNEUROSCI.0006-15.2015
69. Kant S, Stopa EG, Johanson CE, Baird A, Silverberg GD. Choroid plexus genes for CSF production and brain homeostasis are altered in Alzheimer's disease. *Fluids Barriers CNS*. 2018;15:34. doi: 10.1186/s12987-018-0120-7
70. Tadayon E, Pascual-Leone A, Press D, Santarnecchi E. Alzheimer's disease neuroimaging I. Choroid plexus volume is associated with levels of CSF proteins: relevance for Alzheimer's and Parkinson's disease. *Neurobiol Aging*. 2020;89:108-117. doi: 10.1016/j.neurobiolaging.2020.01.005
71. Choi JD, Moon Y, Kim H-J, Yim Y, Lee S, Moon W-J. Choroid plexus volume and permeability at brain MRI within the Alzheimer disease clinical spectrum. *Radiology*. 2022;304:635-645. doi: 10.1148/radiol.212400
72. Sala-Llonch R, Idland A-V, Borza T, et al. Inflammation, amyloid, and atrophy in the aging brain: relationships with longitudinal changes in cognition. *J Alzheimers Dis*. 2017;58:829-840. doi: 10.3233/JAD-161146
73. Racine AM, Merluzzi AP, Adluru N, et al. Association of longitudinal white matter degeneration and cerebrospinal fluid biomarkers of neurodegeneration, inflammation and Alzheimer's disease in late-middle-aged adults. *Brain Imaging Behav*. 2019;13:41-52. doi: 10.1007/s11682-017-9732-9
74. Hu WT, Howell JC, Ozturk T, et al. CSF Cytokines in aging, multiple sclerosis, and dementia. *Front Immunol*. 2019;10:480. doi: 10.3389/fimmu.2019.00480
75. Brosseron F, Kolbe C-C, Santarelli F, et al. Multicenter Alzheimer's and Parkinson's disease immune biomarker verification study. *Alzheimers Dement*. 2020;16:292-304. doi: 10.1016/j.jalz.2019.07.018
76. Craig-Schapiro R, Perrin RJ, Roe CM, et al. YKL-40: a novel prognostic fluid biomarker for preclinical Alzheimer's disease. *Biol Psychiatry*. 2010;68:903-912. doi: 10.1016/j.biopsych.2010.08.025
77. Taipa R, Das Neves SP, Sousa AL, et al. Proinflammatory and anti-inflammatory cytokines in the CSF of patients with Alzheimer's disease and their correlation with cognitive decline. *Neurobiol Aging*. 2019;76:125-132. doi: 10.1016/j.neurobiolaging.2018.12.019
78. Rauchmann B-S, Schneider-Axmann T, Alexopoulos P, Perneczky R. Alzheimer's Disease Neuroimaging, I. CSF soluble TREM2 as a measure of immune response along the Alzheimer's disease continuum. *Neurobiol Aging*. 2019;74:182-190. doi: 10.1016/j.neurobiolaging.2018.10.022
79. Rauchmann B-S, Sadlon A, Perneczky R. Alzheimer's disease neuroimaging, I. Soluble TREM2 and inflammatory proteins in Alzheimer's disease cerebrospinal fluid. *J Alzheimers Dis*. 2020;73:1615-1626. doi: 10.3233/JAD-191120
80. Llorens F, Thüne K, Tahir W, et al. YKL-40 in the brain and cerebrospinal fluid of neurodegenerative dementias. *Mol Neurodegener*. 2017;12:83. doi: 10.1186/s13024-017-0226-4
81. Gate D, Saligrama N, Leventhal O, et al. Clonally expanded CD8 T cells patrol the cerebrospinal fluid in Alzheimer's disease. *Nature*. 2020;577:399-404. doi: 10.1038/s41586-019-1895-7
82. Higginbotham L, Ping L, Dammer EB, et al. Integrated proteomics reveals brain-based cerebrospinal fluid biomarkers in asymptomatic and symptomatic Alzheimer's disease. *Sci Adv*. 2020;6:eaaz9360. doi: 10.1126/sciadv.aaz9360
83. Johnson ECB, Dammer EB, Duong DM, et al. Large-scale proteomic analysis of Alzheimer's disease brain and cerebrospinal fluid reveals early changes in energy metabolism associated with microglia and astrocyte activation. *Nat Med*. 2020;26:769-780. doi: 10.1038/s41591-020-0815-6
84. Nathan C. Points of control in inflammation. *Nature*. 2002;420:846-852. doi: 10.1038/nature01320
85. Chen CPC, Chen RL, Preston JE. The influence of ageing in the cerebrospinal fluid concentrations of proteins that are derived from the choroid plexus, brain, and plasma. *Exp Gerontol*. 2012;47:323-328. doi: 10.1016/j.exger.2012.01.008

86. Hampel H, Teipel SJ, Padberg F, et al. Discriminant power of combined cerebrospinal fluid tau protein and of the soluble interleukin-6 receptor complex in the diagnosis of Alzheimer's disease. *Brain Res*. 1999;823:104-112. doi: 10.1016/s0006-8993(99)01146-4
87. Angel TE, Jacobs JM, Smith RP, et al. Cerebrospinal fluid proteome of patients with acute Lyme disease. *J Proteome Res*. 2012;11:4814-4822. doi: 10.1021/pr300577p
88. Collins MA, An J, Hood BL, Conrads TP, Bowser RP. Label-free LC-MS/MS proteomic analysis of cerebrospinal fluid identifies protein/pathway alterations and candidate biomarkers for amyotrophic lateral sclerosis. *J Proteome Res*. 2015;14:4486-4501. doi: 10.1021/acs.jproteome.5b00804
89. Gromicho M, Pronto-Laborinho A, Almeida C, et al. Cerebrospinal fluid chitinases as biomarkers for amyotrophic lateral sclerosis. *Diagnostics (Basel)*. 2021;11:1210. doi: 10.3390/diagnostics11071210
90. Jorm AF, Jolley D. The incidence of dementia: a meta-analysis. *Neurology*. 1998;51:728-733. doi: 10.1212/wnl.51.3.728
91. Albrecht DS, Sagare A, Pachicano M, et al. Early neuroinflammation is associated with lower amyloid and tau levels in cognitively normal older adults. *Brain Behav Immun*. 2021;94:299-307. doi: 10.1016/j.bbi.2021.01.010
92. Bettcher BM, Johnson SC, Fitch R, et al. Cerebrospinal fluid and plasma levels of inflammation differentially relate to CNS markers of Alzheimer's disease pathology and neuronal damage. *J Alzheimers Dis*. 2018;62:385-397. doi: 10.3233/JAD-170602
93. Iram T, Kern F, Kaur A, et al. Young CSF restores oligodendrogenesis and memory in aged mice via Fgf17. *Nature*. 2022;605:509-515. doi: 10.1038/s41586-022-04722-0
94. Gorbunova V, Seluanov A, Kennedy BK. The World goes bats: living longer and tolerating viruses. *Cell Metab*. 2020;32:31-43. doi: 10.1016/j.cmet.2020.06.013
95. Bergen AA, Kaing S, Ten Brink JB, Gorgels TG, Janssen SF. Gene expression and functional annotation of human choroid plexus epithelium failure in Alzheimer's disease. *BMC Genomics*. 2015;16:956. doi: 10.1186/s12864-015-2159-z
96. Fame RM, Lehtinen MK. Emergence and developmental roles of the cerebrospinal fluid system. *Dev Cell*. 2020;52:261-275. doi: 10.1016/j.devcel.2020.01.027
97. May C, Kaye JA, Atack JR, Schapiro MB, Friedland RP, Rapoport SI. Cerebrospinal fluid production is reduced in healthy aging. *Neurology*. 1990;40:500-503. doi: 10.1212/wnl.40.3_part_1.500
98. Silverberg GD, Heit G, Huhn S, et al. The cerebrospinal fluid production rate is reduced in dementia of the Alzheimer's type. *Neurology*. 2001;57:1763-1766. doi: 10.1212/wnl.57.10.1763
99. Silverberg GD, Mayo M, Saul T, Rubenstein E, McGuire D, et al. Alzheimer's disease, normal-pressure hydrocephalus, and senescent changes in CSF circulatory physiology: a hypothesis. *Lancet Neurol*. 2003;2:506-511. doi: 10.1016/s1474-4422(03)00487-3
100. Silverberg G, Mayo M, Saul T, Fellmann J, Mcguire D. Elevated cerebrospinal fluid pressure in patients with Alzheimer's disease. *Cerebrospinal Fluid Res*. 2006;3:7. doi: 10.1186/1743-8454-3-7
101. Tarkowski E. Intrathecal inflammation precedes development of Alzheimer's disease. *J Neurol Neurosurg Psychiatry*. 2003;74:1200-1205. doi: 10.1136/jnnp.74.9.1200
102. Nathan C, Ding A. Nonresolving inflammation. *Cell*. 2010;140:871-882. doi: 10.1016/j.cell.2010.02.029
103. Marques F, Sousa JC, Coppola G, et al. The choroid plexus response to a repeated peripheral inflammatory stimulus. *BMC Neurosci*. 2009;10:135. doi: 10.1186/1471-2202-10-135
104. Carloni S, Bertocchi A, Mancinelli S, et al. Identification of a choroid plexus vascular barrier closing during intestinal inflammation. *Science*. 2021;374:439-448. doi: 10.1126/science.abc6108
105. Cui J, Shipley FB, Shannon ML, et al. Inflammation of the embryonic choroid plexus barrier following maternal immune activation. *Dev Cell*. 2020;55:617-628. doi: 10.1016/j.devcel.2020.09.020
106. Hur Ji-Y, Frost GR, Wu X, et al. The innate immunity protein IFITM3 modulates gamma-secretase in Alzheimer's disease. *Nature*. 2020;586:735-740. doi: 10.1038/s41586-020-2681-2
107. Heneka MT, Mcmanus RM, Latz E. Inflammasome signalling in brain function and neurodegenerative disease. *Nat Rev Neurosci*. 2018;19:610-621. doi: 10.1038/s41583-018-0055-7
108. Wightman DP, Jansen IE, Savage JE, et al. A genome-wide association study with 1,126,563 individuals identifies new risk loci for Alzheimer's disease. *Nat Genet*. 2021;53:1276-1282. doi: 10.1038/s41588-021-00921-z
109. Jack CR, Bennett DA, Blennow K, et al. Toward a biological definition of Alzheimer's disease. *Alzheimers Dement*. 2018;14:535-562. doi: 10.1016/j.jalz.2018.02.018
110. Braak H, Braak E. Neuropathological stageing of Alzheimer-related changes. *Acta Neuropathol*. 1991;82:239-259. doi: 10.1007/BF00308809
111. Benson MD, Smith RA, Hung G, et al. Suppression of choroid plexus transthyretin levels by antisense oligonucleotide treatment. *Amyloid*. 2010;17:43-49. doi: 10.3109/13506129.2010.483121
112. Smith R, Myers K, Ravits J, Bowser R. Amyotrophic lateral sclerosis: is the spinal fluid pathway involved in seeding and spread? *Med Hypotheses*. 2015;85:576-583. doi: 10.1016/j.mehy.2015.07.014
113. Dani N, Herbst RH, Mccabe C, et al. A cellular and spatial map of the choroid plexus across brain ventricles and ages. *Cell*. 2021;184:3056-3074. doi: 10.1016/j.cell.2021.04.003
114. Szmydynger-Chodobska J, Chodobski A, Johanson CE. Postnatal developmental changes in blood flow to choroid plexuses and cerebral cortex of the rat. *Am J Physiol*. 1994;266:R1488-1492. doi: 10.1152/ajpregu.1994.266.5.R1488
115. Stopa EG, Tanis KQ, Miller MC, et al. Comparative transcriptomics of choroid plexus in Alzheimer's disease, frontotemporal dementia and Huntington's disease: implications for CSF homeostasis. *Fluids Barriers CNS*. 2018;15:18. doi: 10.1186/s12987-018-0102-9
116. González-Marrero I, Castañeyra-Ruiz L, González-Toledo JM, et al. High blood pressure effects on the blood to cerebrospinal fluid barrier and cerebrospinal fluid protein composition: a two-dimensional electrophoresis study in spontaneously hypertensive rats. *Int J Hypertens*. 2013;2013:164653. doi: 10.1155/2013/164653
117. Pellegrini L, Bonfio C, Chadwick J, Begum F, Skehel M, Lancaster MA. Human CNS barrier-forming organoids with cerebrospinal fluid production. *Science*. 2020;369:eaaz5626. doi: 10.1126/science.aaz5626
118. Sweeney MD, Kisler K, Montagne A, Toga AW, Zlokovic BV. The role of brain vasculature in neurodegenerative disorders. *Nat Neurosci*. 2018;21:1318-1331. doi: 10.1038/s41593-018-0234-x
119. Montagne A, Barnes SR, Sweeney MD, et al. Blood-brain barrier breakdown in the aging human hippocampus. *Neuron*. 2015;85:296-302. doi: 10.1016/j.neuron.2014.12.032
120. Gião T, Saavedra J, Vieira JR, Pinto MT, Arsequell G, Cardoso I. Neuroprotection in early stages of Alzheimer's disease is promoted by transthyretin angiogenic properties. *Alzheimers Res Ther*. 2021;13:143. doi: 10.1186/s13195-021-00883-8
121. Zhou S, Davidson C, Mcglynn R, et al. Endosomal/lysosomal processing of gangliosides affects neuronal cholesterol sequestration in Niemann-Pick disease type C. *Am J Pathol*. 2011;179:890-902. doi: 10.1016/j.ajpath.2011.04.017
122. Peake KB, Vance JE. Defective cholesterol trafficking in Niemann-Pick C-deficient cells. *FEBS Lett*. 2010;584:2731-2739. doi: 10.1016/j.febslet.2010.04.047
123. Sheardova K, Vyhnalek M, Nedelska Z, et al. Czech Brain Aging Study (CBAS): prospective multicentre cohort study on risk and protective factors for dementia in the Czech Republic. *BMJ Open*. 2019;9:e030379. doi: 10.1136/bmjopen-2019-030379
124. Russo MJ, Gustafson D, Vázquez S, et al. Creation of the Argentina-Alzheimer's Disease Neuroimaging Initiative. *Alzheimers Dement*. 2014;10:S84-87. doi: 10.1016/j.jalz.2013.09.015

125. Saul J, Hutchins E, Reiman R, et al. Global alterations to the choroid plexus blood-CSF barrier in amyotrophic lateral sclerosis. *Acta Neuropathol Commun*. 2020;8:92. doi: 10.1186/s40478-020-00968-9
126. Ruffmann C, Calboli FCF, Bravi I, et al. Cortical Lewy bodies and Abeta burden are associated with prevalence and timing of dementia in Lewy body diseases. *Neuropathol Appl Neurobiol*. 2016;42:436-445. doi: 10.1111/nan.12294
127. Vanderstichele H, Bibl M, Engelborghs S, et al. Standardization of preanalytical aspects of cerebrospinal fluid biomarker testing for Alzheimer's disease diagnosis: a consensus paper from the Alzheimer's Biomarkers Standardization Initiative. *Alzheimers Dement*. 2012;8:65-73. doi: 10.1016/j.jalz.2011.07.004
128. Prokopenko I, Miyakawa G, Zheng B, et al. Alzheimer's disease pathology explains association between dementia with Lewy bodies and APOE-epsilon4/TOMM40 long poly-T repeat allele variants. *Alzheimers Dement (N Y)*. 2019;5:814-824. doi: 10.1016/j.trci.2019.08.005
129. Shinohara RT, Sweeney EM, Goldsmith J, et al. Statistical normalization techniques for magnetic resonance imaging. *Neuroimage Clin*. 2014;6:9-19. doi: 10.1016/j.nicl.2014.08.008
130. Desikan RS, Ségonne F, Fischl B, et al. An automated labeling system for subdividing the human cerebral cortex on MRI scans into gyral based regions of interest. *Neuroimage*. 2006;31:968-980. doi: 10.1016/j.neuroimage.2006.01.021
131. Fischl B, Salat DH, Busa E, et al. Whole brain segmentation: automated labeling of neuroanatomical structures in the human brain. *Neuron*. 2002;33:341-355. doi: 10.1016/s0896-6273(02)00569-x
132. Reuter M, Schmansky NJ, Rosas HD, Fischl B. Within-subject template estimation for unbiased longitudinal image analysis. *Neuroimage*. 2012;61:1402-1418. doi: 10.1016/j.neuroimage.2012.02.084
133. Nikolaeva S, Bayunova L, Sokolova T, et al. GM1 and GD1a gangliosides modulate toxic and inflammatory effects of E. coli lipopolysaccharide by preventing TLR4 translocation into lipid rafts. *Biochim Biophys Acta*. 2015;1851:239-247. doi: 10.1016/j.bbalip.2014.12.004
134. Teipel StJ, Pruessner JC, Faltraco F, et al. Comprehensive dissection of the medial temporal lobe in AD: measurement of hippocampus, amygdala, entorhinal, perirhinal and parahippocampal cortices using MRI. *J Neurol*. 2006;253:794-800. doi: 10.1007/s00415-006-0120-4
135. Seab JP, Jagust WJ, Wong STS, Roos MS, Reed BR, Budinger TF. Quantitative NMR measurements of hippocampal atrophy in Alzheimer's disease. *Magn Reson Med*. 1988;8:200-208. doi: 10.1002/mrm.1910080210
136. Zdanovskis N, Platkājis A, Kostiks A, Grigorjeva O, Karelis G. Cerebellar cortex and cerebellar white matter volume in normal cognition, mild cognitive impairment, and dementia. *Brain Sci*. 2021;11:1134. doi: 10.3390/brainsci11091134
137. Monereo-Sánchez J, De Jong JJA, Drenthen GS, et al. Quality control strategies for brain MRI segmentation and parcellation: practical approaches and recommendations - insights from the Maastricht study. *Neuroimage*. 2021;237:118174. doi: 10.1016/j.neuroimage.2021.118174

SUPPORTING INFORMATION

Additional supporting information can be found online in the Supporting Information section at the end of this article.

How to cite this article: Čarna M, Onyango IG, Katina S, et al. Pathogenesis of Alzheimer's disease: Involvement of the choroid plexus. *Alzheimer's Dement*. 2023;1-18. https://doi.org/10.1002/alz.12970